

SUPPLEMENTAL MATERIAL

Expanded Methods:

Study subjects:

The study was performed at the Johns Hopkins Hospital, approved by its Institutional Review Board, and all participants provided written consent. Twenty-seven patients (age = 45 ± 14 yrs, mean \pm SD) with a history of HF (New York Heart Association, NYHA, class I-III) and reduced LV EF ($\leq 45\%$) measured at a prior clinical imaging study using echocardiography, nuclear ventriculography, x-ray computed tomography (CT) or MRI were enrolled, as previously described.¹⁴ Participants were excluded who had contraindications to MRI, significant valvular disease, or evidence of significant coronary disease (luminal stenosis $> 50\%$ as assessed by cardiac catheterization, CT angiography, or positive stress nuclear or echocardiography). Fourteen age-matched healthy subjects (age = 42 ± 18 yrs) with no history of heart disease, diabetes, or hypertension were enrolled as controls. The initial report of these subjects focused on cardiac work and contractile abnormalities and contained additional demographic information.¹⁴ The data were subsequently analyzed to test for a relationship between altered energy metabolism and adverse remodeling and that previously unpublished analysis appears here.

Human cardiac MRS and MRI:

All cardiac MRI and MRS studies were performed on a 3 Tesla scanner (Achieva, *Philips Healthcare*, Best, the Netherlands) equipped with 6- and 32-channel cardiac array coils and a 17-cm/8-cm custom ³¹P transmit/receive surface coil set.⁶⁶ Spatially-localized ³¹P MRS measured concentrations of [PCr] and [ATP] in $\mu\text{mol/g}$ wet weight in the left anterior ventricle were obtained from metabolite peak areas and an external concentration reference quantified using the 'Circle Fit' method.⁶⁶ Concentrations were corrected for coil loading, relaxation, heart motion, tissue volume, [ATP] in ventricular blood, and coil sensitivity variations within voxels.⁶⁶ The pseudo-first-order rate-constant of the CK reaction, k_f in s^{-1} , was measured using the triple repetition-time saturation-transfer (TRiST) method⁶⁷ with corrections for spillover irradiation.^{68,69} The CK flux was calculated from the product, k_f [PCr], and reported as $\mu\text{mol/g/s}$.

Cine MRI was performed with participants positioned either supine and scanned with 6- or 32-channel cardiac array coils, or prone using the scanner's body MRI coil. Double-oblique short-axis retrospective cardiac-gated MRI was performed in breath-hold acquisitions using balanced steady-state free precession (SSFP; 8-12 slices; TR=3.5 ms; echo time TE=1.8 ms; 30 cardiac phases; slice thickness=8 mm; slice gap=2mm; SENSE factor=2 for coil arrays; 1.6x1.3 mm in-plane scan resolution; 256x256 matrix; 1-2 slices/breath-hold; 15-25 min total MRI exam time). The inner and outer contours of the LV were manually delineated in all short-axis MRI sections at all time points. The LV mass was calculated from the difference between the two contours at end-diastole summed over all slices and multiplied by specific gravity. The LV blood volume was calculated at each cardiac phase by summing the blood volumes in all adjacent myocardial sections.¹⁴

Murine *in vivo* cardiac MRI and MRS:

In vivo MRI/MRS experiments were performed on a Bruker spectrometer equipped with a 4.7-T/40-cm Oxford magnet and actively shielded gradients using techniques previously described.¹⁵ Briefly, a complete set of high temporal and spatial resolution multi-slice cine MR images was acquired of the entire LV without gaps to assess LV mass, ventricular volumes, and EF.^{70,71} A one-dimensional ³¹P chemical shift imaging sequence was used to obtain HEP data. The PCr and ATP peaks in ³¹P MRS were quantified by integration of the peak areas determined by an investigator blinded to genotype and group assignment (by use of ID codes that did not reveal

genotype or surgical intervention) and the absolute concentrations of PCr and ATP determined using an external concentration reference as described previously.¹⁰ To measure the rate of ATP synthesis through cardiac CK, separate spatially localized TRiST MRS studies were performed in some animals using a previously published protocol, again with peak areas determined by an investigator blinded to genotype and group assignment.⁶⁷

Transgenic mouse lines:

All transgenic mouse development work was performed at the transgenic core facility of UCLA. Transgenic mice were created on the basis of the Tet-off system.⁷² First, two types of mice were generated: first, those with a transgene for the regulatory protein tTA (tetracycline-controlled transactivator) under the control of the α -MHC promoter; and second, mice expressing the CKmito transgene under the control of tetracycline-responsive element (TRE) following microinjection of the CKmito construct into fertilized mouse embryos (C57BL/6 strain). After the crossing of TRE-CKmito mice with α -MHCtTA mice, double transgenic mice (CKmito-tTA) were confirmed by genotyping, and CKmito transgene induction was achieved by a diet free of doxycycline (designated CKmito overexpressors). Control mice were littermates containing either the tTA or CKmito transgene alone. Guanidinoacetate N-methyltransferase knock-out (GAMT^{-/-}) mice were provided as a gift from Dr. Isbrandt and were created as previously described.²⁰ Homozygous GAMT^{-/-} mice were used and compared to WT or heterozygous GAMT mice as controls. Mice were housed according to phenotype for at least six weeks before the start of the study to prevent Cr intake resulting from coprophagia from control littermates.

Interventions to induce in vivo hypertrophy/heart failure:

Animals were assigned an alphanumeric code so that investigators were blinded to the genetic background of each mouse. Eight to 16-week-old male mice underwent sham or TAC surgery as previously described.^{5,15} Studies were performed in male mice to limit the variation in remodeling and functional response to pressure overload. Female mice exhibit attenuated remodeling relative to males.⁷³ As we aimed to quantitatively image remodeling in heart failure, the more severe disease in male mice was better suited to these studies. Prior studies had shown that this method of TAC results in cardiac dilatation and dysfunction, as well as a reduction in cardiac PCr/ATP ratio and ATP flux through CK of a magnitude similar to that in human heart failure.^{5,12,15} From all of these studies of more than 178 TAC hearts, only five TAC hearts were excluded that did not exhibit hypertrophy (LV mass) and dysfunction (EF) of 2SD beyond mean of sham hearts, as done previously by others^{74,75}. In additional studies, experiments were performed at 2-3 weeks post-TAC or sham surgery as indicated in the figure legends. Chronic isoproterenol administration was accomplished by subcutaneous implantation of Alzet osmotic mini-pumps (model 1004, Durect Corporation, Cupertino, CA, US) containing either 0.0125mg/kg of isoproterenol or saline. Assignments of mice to the TAC or non-TAC surgery groups as well as to chronic isoproterenol or saline mini-pump implantation groups among littermates or comparable aged litters were done randomly by an investigator not performing these operations. All the animal procedures and protocols were reviewed and approved by the Institutional Animal Care and Use Committee of the Johns Hopkins University.

Isolated Myocyte Studies:

Cardiomyocytes were freshly isolated from mice nine weeks after sham or TAC surgery, and sarcomere shortening and whole Ca²⁺ transients were assessed as described previously.^{76,77} Briefly, at the start of each experiment, the cells were field-stimulated continuously for 10-15 min to establish contractile stability. Recording of twitch amplitude started during the stabilization period, and cell shortening data were collected through the whole experiment. Cells were imaged using field-stimulation (Warner Instruments) in an inverted fluorescence microscope. The cells

were superfused with Tyrode's solution, and the test solutions were rapidly switched. Stable cells were used to examine the effects of all the interventions on myocyte contractility (each in separate groups of cells). The cardiomyocytes were superfused with isoproterenol (ISO, 2.5 nM, 10 min) to assess the extent of stimulation. Sarcomere length was measured by real-time Fourier transform, and whole calcium transient by xenon excitation of Fura 2 fluorescence in a dark room. Steady-state twitches and Ca^{2+} transients were averaged over 30 s periods. Twitch amplitude was expressed as a percentage of resting sarcomere length. To determine myocyte survival after acute oxidative stress, the cells were infused with H_2O_2 (50 μM , for 700 sec) and the time interval between the onset of H_2O_2 superfusion and the appearance of an irreversible arrhythmia was measured.

Measurement of reactive oxygen species (ROS) by electronic paramagnetic resonance (EPR) spectroscopy:

ROS measurements were conducted as previously described.⁷⁸ Briefly, LV tissue freshly isolated from sham or 9-week TAC mice were homogenized in phosphate-buffered saline (PBS) containing 0.1 mM diethylenetriaminepentaacetic acid (DTPA) and protease inhibitor cocktail (Roche Applied Science, Indianapolis, IN) at pH 7.4. Insoluble fractions were removed by centrifugation at 15000 x g for 10 min at 4 °C. Stock solutions of 1-hydroxy-3-methoxycarbonyl-2,2,5,5-tetramethylpyrrolidine hydrochloride (CMH; Enzo Life Sciences, Farmingdale, NY) were prepared daily in nitrogen-purged 0.9% (w/v) NaCl, 25 g/L Chelex 100 (Bio-Rad) and 0.1 mM DTPA, and kept on ice.⁷⁸ The samples were treated with 1 mM CMH at 37 °C for 2 min, transferred to 0.05 ml glass capillary tubes, and analyzed on a Bruker E-Scan (Billerica, MA) electron paramagnetic resonance (EPR) spectrometer. Spectrometer settings were as follows: sweep width, 100 G; microwave frequency, 9.75 GHz; modulation amplitude, 1 G; conversion time, 5.12 ms; receiver gain, 2×10^3 ; the number of scans, 16. EPR signal intensities were normalized to the protein concentrations of the tissue homogenates determined by Pierce BCA protein assay kit (Life Technologies).

Isolated Mitochondria Studies:

Heart mitochondria were freshly isolated from mice nine weeks after sham or TAC surgery, and mitochondrial respiration was assayed on a high-throughput automated 96-well extracellular flux analyzer (Seahorse XF96; Seahorse Bioscience, Billerica, MA) as previously described.^{79,80} Briefly, mitochondria (the equivalent of 5–15 mg mitochondrial protein) were transferred to each well and the oxygen consumption rate (OCR) of the different complexes of the respiratory chain was evaluated with substrates of complex I, II, and IV in the assay buffer (137 mM KCl, 2 mM KH_2PO_4 , 0.5 mM EGTA, 2.5 mM MgCl_2 , and 20 mM HEPES containing 0.2% fatty acid-free bovine serum albumin) at pH 7.2 and 37°C. State 2 and State 3 respiratory capacity was analyzed in the absence or presence of ADP (1 mM). In a separate experiment, proton leak was assessed by measuring basal oxygen consumption rate after blocking the F_0F_1 ATPase with oligomycin A (1 μM), followed by determination of maximal uncoupled respiration with FCCP (1 μM). OCRs were normalized to the mitochondrial protein concentrations determined by the Pierce BCA protein assay kit (Life Technologies). Mitochondrial ROS levels were monitored by using MitoSOX probe as described previously.⁸⁰

Thioredoxin reductase (TrxR) activity assays:

Total TrxR activity assay was performed as previously described.²² Stock solutions of NADPH (48 mM) and 5,5'-dithio-bis-[2-nitrobenzoic acid] (DTNB, 100 mM) were prepared in MilliQ water and DMSO, respectively. Flash-frozen left ventricular heart tissue from sham or 9-week TAC mice were homogenized in 0.1 M potassium phosphate buffer containing 0.1 mM DTPA and protease inhibitor cocktail at pH 7.0. The samples were then subjected to three sequential freeze/thaw cycles between liquid nitrogen and a 37 °C water bath. The insoluble fractions were removed by

centrifugation at 14000 x g for 2 min at 4 °C. The protein concentrations were quantified by BCA assay (Pierce). Total TrxR activities were determined as described previously.²² Briefly, the homogenates (0.1 mg/ml total protein) were incubated with 0.24 mM NADPH and 3 mM DTNB in pH 7.0 potassium phosphate buffer in the presence or absence of thioredoxin reductase inhibitor, auranofin (100 nM) for 2 h at room temperature (in the dark). The relative absorbances of 2-nitro-5-thiobenzoate anion (TNB²⁻, $\epsilon_{412}=14150 \text{ M}^{-1}\text{cm}^{-1}$) were detected on a SpectraMax microplate reader (Molecular Devices) at baseline and following two hour incubation. In all cases, each sample was analyzed in triplicate, and total TrxR activity was calculated.

Citrate synthase (CS) activity assays:

Stock solutions of oxaloacetic acid (10 mM) and DTNB (1 mM) were prepared daily in 50 mM Tris-HCl buffer (pH 8.0) and stored in ice. Stock solutions of acetyl-coenzyme A (CoA) were prepared in MilliQ water. Flash-frozen murine heart tissue was homogenized in pH 8 Tris-HCl buffer containing 0.25% Triton X-100 and protease inhibitor cocktail. The insoluble fractions were removed by centrifugation at 15000xg for 10 min at 4°C. The protein concentrations were quantified by BCA assay (Pierce). CS activity was determined by using a modified literature procedure.⁸¹ Briefly, the CS reaction was initiated by adding homogenates containing CoA to a reaction mixture to yield a final concentration of 25 ug/ml total protein, 0.3 mM CoA, 0.1 mM DTNB, and 0.5 mM oxaloacetic acid in pH 8 Tris-HCl buffer. The samples were incubated at room temperature for 30 min (in the dark). The relative absorbances of 2-nitro-5-thiobenzoate anion (TNB²⁻, $\epsilon_{412}=14150 \text{ M}^{-1}\text{cm}^{-1}$) were detected on a SpectraMax microplate reader (Molecular Devices) at baseline and following 30 min incubation. In all cases, the samples were analyzed in duplicate, and CS activity was calculated.

Electrophoresis and Western Blot:

Murine heart tissue was isolated and homogenized in PBS containing 0.1 mM DTPA and protease inhibitor cocktail (pH 7.4). The insoluble fractions were removed by centrifugation at 15000 x g for 10 min at 4 °C, and protein concentrations were determined by BCA assay. All gels and Western blots were run using a Bio-Rad Mini-Protean II electrophoresis and Western blotting system. Samples were prepared in SDS Laemmli buffer and dithiothreitol (DTT, 50 mM). SDS-PAGE using 4-20% polyacrylamide was performed. Upon separation by gel electrophoresis, the proteins were transferred via Western blotting onto nitrocellulose membranes (Li-Cor). The proteins were detected using rabbit polyclonal antibodies anti-CKmito (1:3000 dilution, Abcam, ab198257), anti-TrxR1 (1:1000 dilution, Abcam, ab16840), anti-TrxR2 (1:2000 dilution, Invitrogen, LFPA0024), anti-VDAC1/Porin (1:1000 dilution, Abcam, ab15895), anti-Akt (1:1000 dilution, Cell Signaling, 9272), anti-GATA4 (1:1000 dilution, Abcam, ab84593), anti-Mad1 (1:500 dilution, Cell Signaling, 4682), anti-GPx1 (1:1000 dilution, Abcam, ab59546), anti-pmTOR (1:1000 dilution, Cell Signaling, 2971), anti-mTOR (1:1000 dilution, Cell Signaling, 2972), anti-ERK1/2 (1:1000 dilution, Cell Signaling, 9102), anti-CK-B (1:2000, Millipore Sigma, HPA001254) anti-pGSK3 β (1:1000 dilution, Cell Signaling, 9336), and anti-GSK3 β (1:1000 dilution, Cell Signaling, 9332), rabbit monoclonal antibodies anti-SOD2 (1:1000 dilution, Cell Signaling, 13141), anti-pAkt (1:2000 dilution, Cell Signaling, 4060), anti-FoxO3a (1:1000 dilution, Cell Signaling, 2497), anti-GAPDH (1:1000 dilution, Cell Signaling, 2118), and anti-pERK1/2 (1:2000, Cell Signaling, 4370), and mouse monoclonal antibodies anti-cMyc (1:500 dilution, Invitrogen, 13-2500), anti-CKmyofib (1:1000 dilution, Santa Cruz, sc-365046) and anti-Nrf2 (1:1000 dilution, Santa Cruz, sc-365949). Primary antibody binding was visualized by using the secondary antibodies IRDye 800CW goat anti-rabbit IgG (1:10000 dilution, Li-Cor Biosciences, 926-32211), IRDye 680LT goat anti-rabbit IgG (1:10000 dilution, Li-Cor Biosciences, 926-68021), IRDye 800CW goat anti-mouse IgG (1:10000 dilution, Li-Cor Biosciences, 926-32210), and IRDye 680LT goat anti-mouse IgG (1:10000, Li-Cor

Biosciences, 926-68020). Membranes were scanned on an Odyssey scanner (Li-Cor Biosciences), and the bands were quantified using Image Studio Lite software (version 5.2).

Statistical Analysis:

Graphs were created using GraphPad Prism software (version 8). Data were tested for normality using the Kolmogorov-Smirnov test for normality. If testing suggested the data distribution was not different from a normal distribution, then data were analyzed with SigmaPlot software (version 12.5, Systat Software, Inc.) by two-way ANOVA followed by Tukey's post-hoc multiple comparison test. Comparisons between two groups were performed using two-tailed Student's *t*-test, as indicated in the figure legends. A value of $p < 0.05$ was considered significant. If testing suggested the data were not normally distributed, then data were analyzed with SAS software and overall comparisons were performed with non-parametric Wilcoxon signed rank test, followed by pair-wise, two-sided multiple comparison analysis (Dwass, Steel, Crichlow-Fligner Method) or with R software (version 4.0.2, dunn.test package) and overall comparisons performed with the non-parametric Kruskal-Wallis test, followed by pair-wise, two-sided multiple comparison analysis (Dunn method with Benjamini-Hochberg adjustment for multiple comparisons). For studies with modest sample size ($n < 6$) where normality testing suggested the results were normally distributed, the results of nonparametric testing are also reported in Supplement Table 1 below. For isolated cardiomyocyte studies, the data were analyzed with SAS software employing a generalized estimating equation model to take into account the correlation of within-subject data, as noted in main Figures 3C, 4B-C, and 5D. Relationships between variables in the human data (Figure 1E-H) were analyzed with SAS software using a linear regression model. All data points for MR spectroscopic and imaging studies and biochemical analyses represent individual mice or human participants. For isolated cardiomyocyte studies, independent experiments were conducted on individual cells that were isolated from 2-6 mice per group as described in the figure legends. For isolated mitochondria studies, tissue from at least two mice were combined for each data point and each data point then treated as an independent measure. All statistical analyses are summarized in the Online Table I.

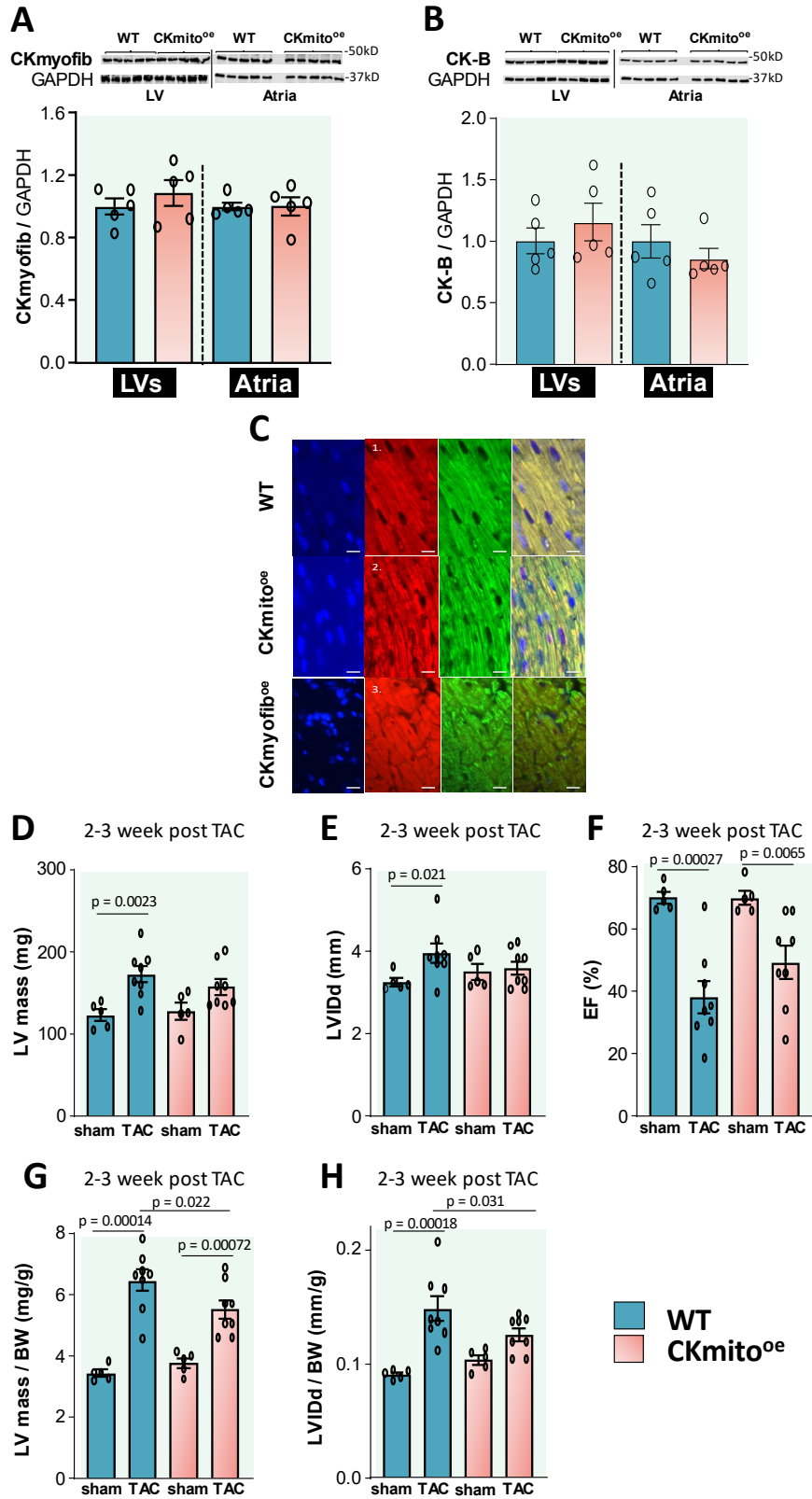


Figure S1. Localization of mitochondrial (CKmito) following cardiac-specific overexpression.

Tissues were isolated from WT and cardiac-specific CKmito overexpressing (CKmito^{oe}) mice. Representative immunoblots and summary of data showing expression levels of **(A)** myofibrillar CK (CKmyofib) and **(B)** brain-type CK (CK-B) normalized to GAPDH (glyceraldehyde-3-phosphate dehydrogenase) and presented as relative to the amount of CKmyofib, or CK-B detected in WT hearts (n=5 per group) **(A-B)**. **(C)** Immunohistochemistry stains for nuclei (blue, left), CKmito (red, panels 1,2), CKmyofib (red, panel 3), mitochondrial marker COXIV (green panel third from left), and overlay image (right). Note that CKmito distribution follows the mitochondrial marker in control and high-expression CKmito overexpressing lines (CKmito^{oe}) and that CKmyofib localization in CKmyofib overexpressing lines (CKmyofib^{oe}) is fundamentally different and in a sarcomeric pattern. The white scale bar in each panel represents 10um. Graphs showing **(D)** left ventricular (LV) mass, **(E)** LV internal end-diastolic diameter (LVIDd), **(F)** ejection fraction (EF), **(G)** the ratio of LV mass to body weight (LV/BW), and **(H)** the ratio of LVIDd to body weight (LVIDd/BW) for WT or CKmito^{oe} mice following 2-3 week post sham operation or thoracic aortic constriction (TAC) as determined by echocardiography (experimental replicates: n=5 (WT sham or CKmito^{oe} sham) and n=8 (WT TAC or CKmito^{oe} TAC) **(E-J)**). Graphs show data points for individual mice. Data were tested for normality using the Kolmogorov-Smirnov test for normality and analyzed by student's t-test **(A)**, Wilcoxon signed rank test **(B)**, or two-way ANOVA followed by Tukey's post-hoc multiple comparison test **(D-H)**. The error bars represent \pm SEM.

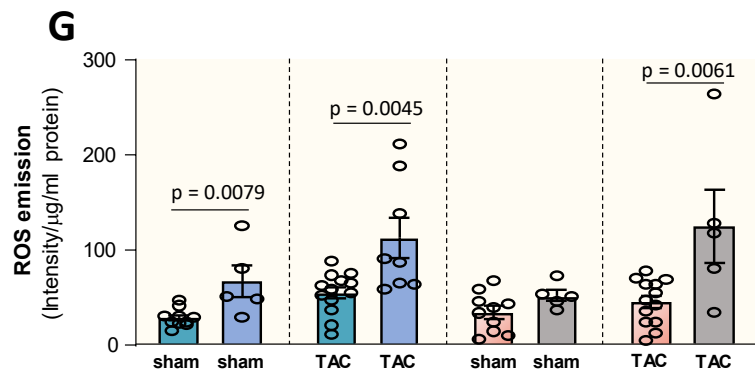
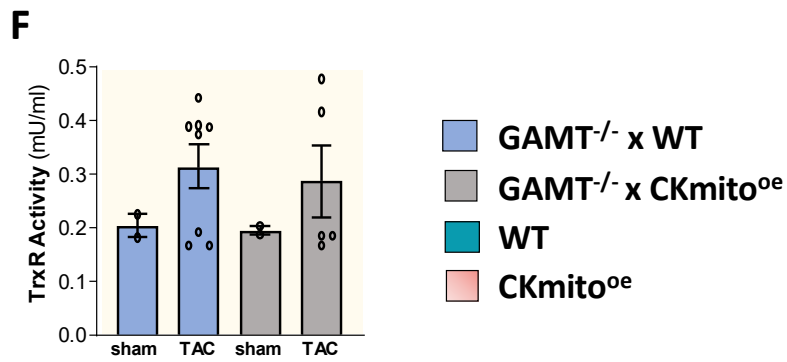
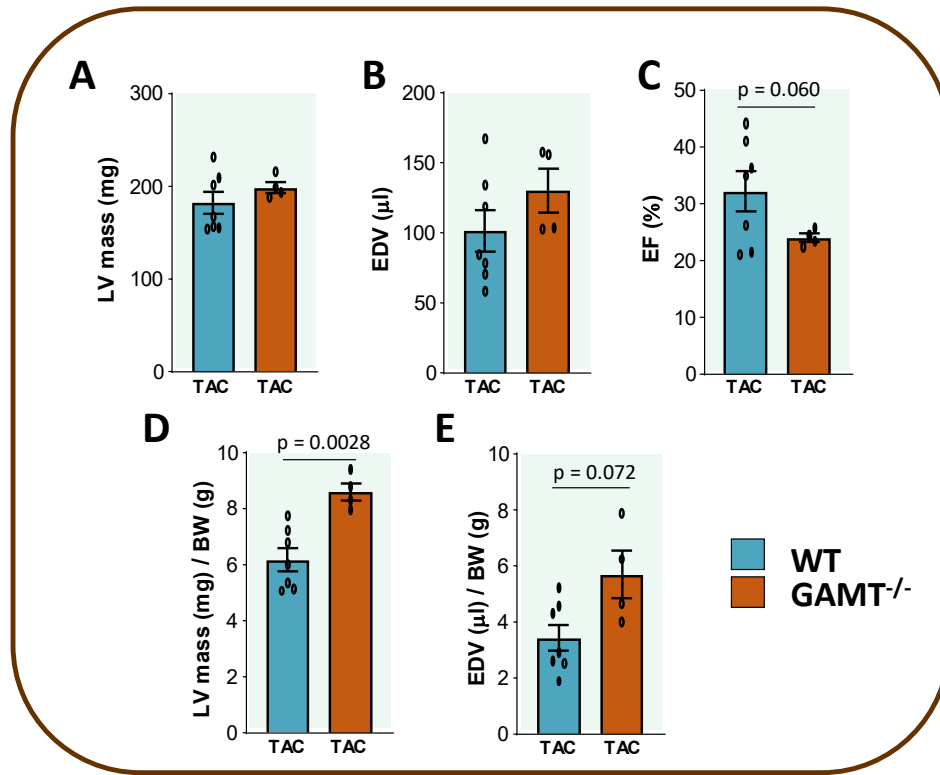


Figure S2. Pathologic remodeling by *in vivo* MRI in creatine-deficient mice ($GAMT^{-/-}$) and reactive oxygen species (ROS) burden in $GAMT^{-/-}$ crossed with mitochondrial creatine kinase overexpressing mice ($GAMT^{-/-}$ x $CKmito^{oe}$) during heart failure. Graphs showing *in vivo* MRI results for **(A)** left ventricular (LV) mass, **(B)** end-diastolic volume (EDV), **(C)** ejection fraction (EF), and the ratios of **(D)** LV mass to body weight (LV mass/BW) and **(E)** EDV to body weight (EDV/BW) for WT or creatine-deficient guanidinoacetate N-methyltransferase knock-out mice ($GAMT^{-/-}$) following thoracic aortic constriction (TAC) (experimental replicates: n=7 (WT TAC) and n=4 ($GAMT^{-/-}$ TAC) **(A-E)**). $GAMT^{-/-}$ were crossed with cardiac-specific CKmito overexpressing ($GAMT^{-/-}$ x $CKmito^{oe}$) or WT ($GAMT^{-/-}$ x WT) mice. **(F)** Graph showing the ratio of heart weight to body weight (HW/BW) following 9-10 week post sham operation or TAC (experimental replicates: n=5 ($GAMT^{-/-}$ x WT sham, $GAMT^{-/-}$ x $CKmito^{oe}$ sham, or $GAMT^{-/-}$ x $CKmito^{oe}$ TAC) and n=8 ($GAMT^{-/-}$ x WT TAC)). **(G)** Thioredoxin reductase (TrxR) activities determined in LV homogenates from $GAMT^{-/-}$ x WT or $GAMT^{-/-}$ x $CKmito^{oe}$ sham or TAC hearts in the presence of excess NADPH (experimental replicates: n=2 ($GAMT^{-/-}$ x WT sham or $GAMT^{-/-}$ x $CKmito^{oe}$ sham), n=8 ($GAMT^{-/-}$ x WT TAC), and n=5 ($GAMT^{-/-}$ x $CKmito^{oe}$ TAC)). **(H)** ROS levels measured by electron paramagnetic resonance (EPR) spectroscopy in LVs of WT, $GAMT^{-/-}$ x WT, $CKmito^{oe}$, and $GAMT^{-/-}$ x $CKmito^{oe}$ sham or TAC hearts (experimental replicates: n=10 (WT sham), n=5 ($GAMT^{-/-}$ x WT sham), n=13 (WT TAC), n=8 ($GAMT^{-/-}$ x WT TAC), n=10 ($CKmito^{oe}$ sham), n=5 ($GAMT^{-/-}$ x $CKmito^{oe}$ sham), n=13 ($CKmito^{oe}$ TAC), and n=5 ($GAMT^{-/-}$ x $CKmito^{oe}$ TAC)). Graphs show data points for individual mice. Data were tested for normality using the Kolmogorov-Smirnov test for normality and analyzed by student's t-test **(A-E, G)** or non-parametric Kruskal-Wallis test, followed by pair-wise, two-sided multiple comparison analysis (Dunn method with Benjamini-Hochberg adjustment) **(F)**. The error bars represent \pm SEM.

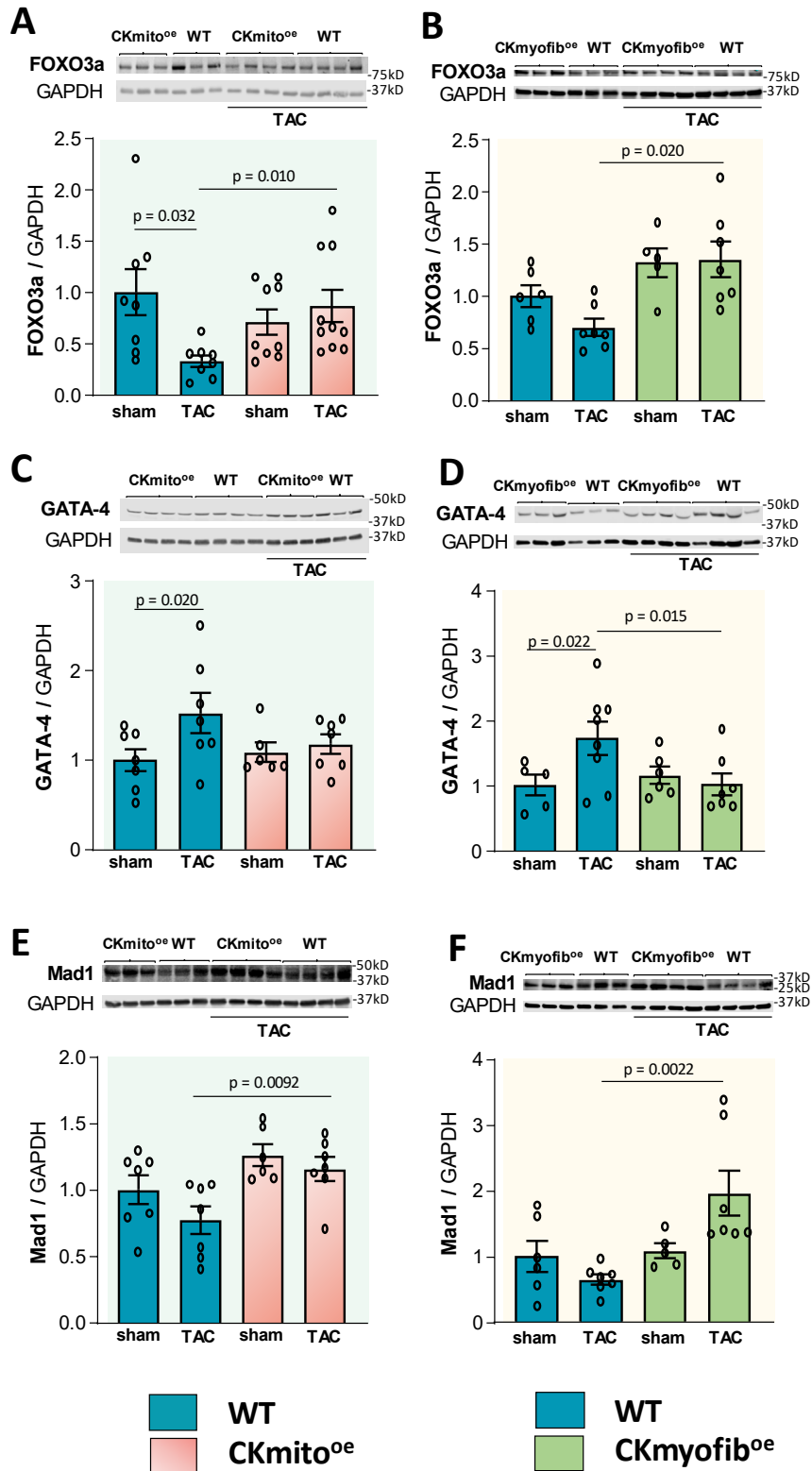


Figure S3. Effect of mitochondrial (CKmito) or myofibrillar creatine kinase (CKmyofib) overexpression on pro-/anti-hypertrophic signaling during TAC heart failure. Left ventricular (LV) tissue from WT or cardiac-specific CKmito (CKmito^{oe}) or CKmyofib overexpressing (CKmyofib^{oe}) sham or TAC hearts were isolated and analyzed. Representative immunoblots and summary of data showing expression levels of **(A, B)** FOXO3a (forkhead box O3), **(C, D)** GATA-4 (transcription factor GATA-4), and **(E, F)** Mad1 (Max dimerization protein 1) in WT, CKmito^{oe} **(A, C, E)**, or CKmyofib^{oe} **(B, D, F)** sham or TAC hearts normalized to GAPDH (glyceraldehyde-3-phosphate dehydrogenase) and presented as relative to the amount of protein detected in sham WT hearts (experimental replicates: n=8 (WT sham or WT TAC), n=9 (CKmito^{oe} sham), and n=10 (CKmito^{oe} TAC) **(A)**; n=6 (WT sham), n=7 (WT TAC or CKmyofib^{oe} TAC), and n=5 (CKmyofib^{oe} sham) **(B)**; n=7 (WT sham, WT TAC, or CKmito^{oe} TAC) and n=6 (CKmito^{oe} sham) **(C)**; n=5 (WT sham), n=8 (WT TAC), n=6 (CKmyofib^{oe} sham), and n=7 (CKmyofib^{oe} TAC) **(D)**; n=7 (WT sham, WT TAC, or CKmito^{oe} TAC) and n=6 (CKmito^{oe} sham) **(E)**; n=6 (WT sham), n=7 (WT TAC, or CKmyofib^{oe} TAC), and n=5 (CKmyofib^{oe} sham) **(F)**). Graphs show data points for individual mice. Data were tested for normality using the Kolmogorov-Smirnov test for normality and analyzed by Wilcoxon signed rank test followed by pair-wise, two-sided multiple comparison analysis (Dwass, Steel, Crichlow-Fligner Method) **(A)**, non-parametric Kruskal-Wallis test, followed by pair-wise, two-sided multiple comparison analysis (Dunn method with Benjamini-Hochberg adjustment) **(B, F)** or two-way ANOVA followed by Tukey's post-hoc multiple comparison test **(C-E)**. The error bars represent \pm SEM.

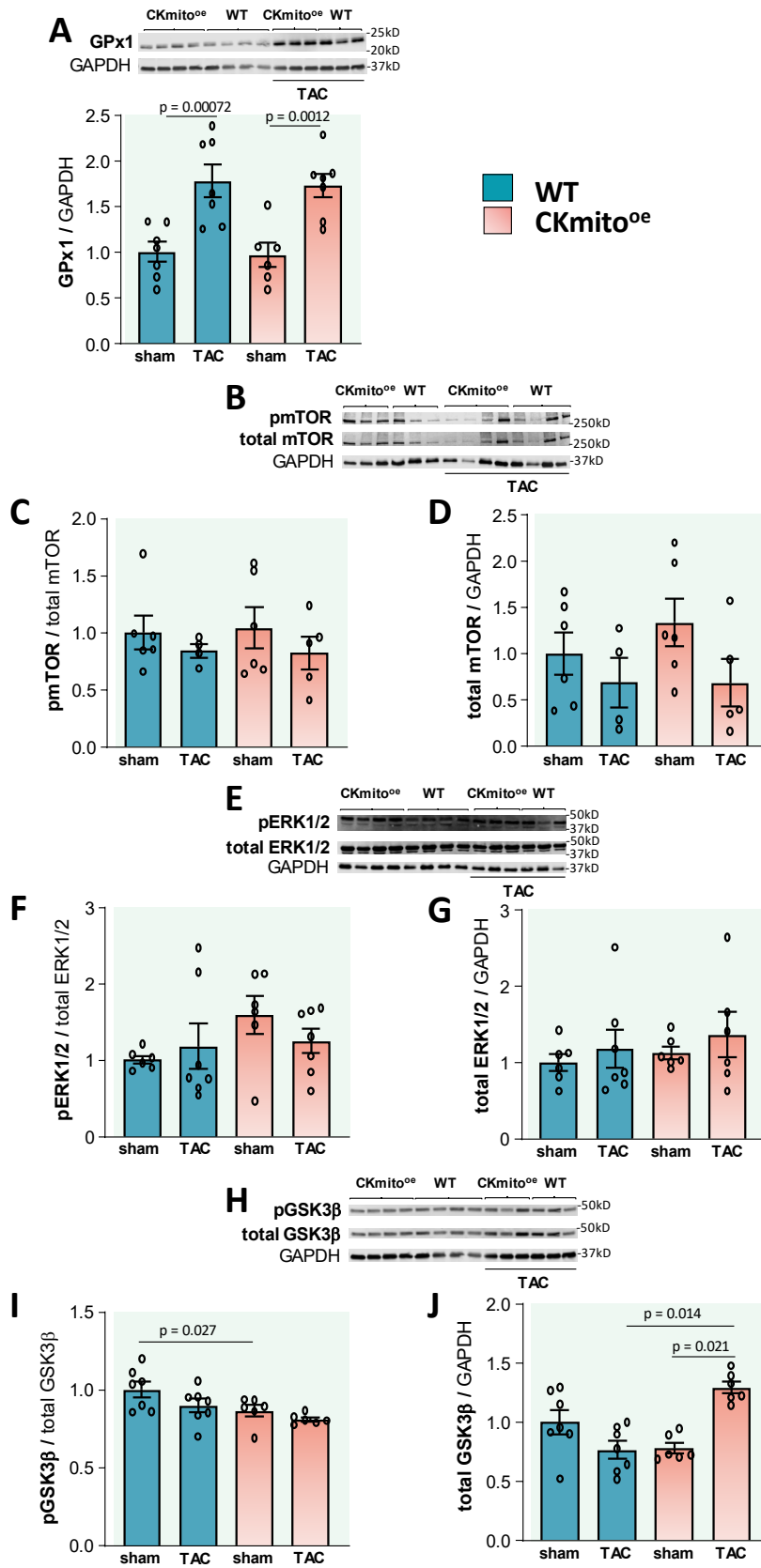


Figure S4. Effect of mitochondrial creatine kinase (CKmito) overexpression on other antioxidant and pro-/anti-hypertrophic signaling pathways in TAC heart failure. Left ventricular (LV) tissue from WT or CKmito overexpressing (CKmito^{oe}) sham or TAC hearts were isolated and analyzed. Representative immunoblots and summary of data showing **(A)** expression levels of GPx1 (glutathione peroxidase 1), **(B, C)** phosphorylation and **(B, D)** expression levels of mTOR (mammalian target of rapamycin), **(E, F)** phosphorylation and **(E, G)** expression levels of ERK (mitogen-activated protein kinase), and **(H, I)** phosphorylation and **(H, J)** expression levels of GSK3 β (glycogen synthase kinase-3 β) normalized to GAPDH (glyceraldehyde-3-phosphate dehydrogenase) **(A, D, G, J)**, total mTOR **(C)**, total ERK **(F)**, or total GSK3 β **(I)**. The data are presented as relative to the amount of protein detected in sham WT hearts (experimental replicates: n=7 (WT sham, WT TAC, or CKmito^{oe} TAC) and n=6 (CKmito^{oe} sham) **(A)**; n=6 (WT sham or CKmito^{oe} sham), n=4 (WT TAC), and n=5 (CKmito^{oe} TAC) **(C-D)**; n=6 (WT sham or CKmito^{oe} sham) and n=7 (WT TAC or CKmito^{oe} TAC) **(F)**; n=6 (WT sham, CKmito^{oe} sham, or CKmito^{oe} TAC) and n=7 (WT TAC) **(G)**; n=7 (WT sham or WT TAC) and n=6 (CKmito^{oe} sham or CKmito^{oe} TAC) **(I-J)**). Graphs show data points for individual mice. Data were tested for normality using the Kolmogorov-Smirnov test for normality and analyzed by two-way ANOVA followed by Tukey's post-hoc multiple comparison test **(A, D, G, I)**, non-parametric Kruskal-Wallis test, followed by pair-wise, two-sided multiple comparison analysis (Dunn method with Benjamini-Hochberg adjustment) **(C)**, or Wilcoxon signed rank test followed by pair-wise, two-sided multiple comparison analysis (Dwass, Steel, Crichlow-Fligner Method) **(F, J)**. The error bars represent \pm SEM.

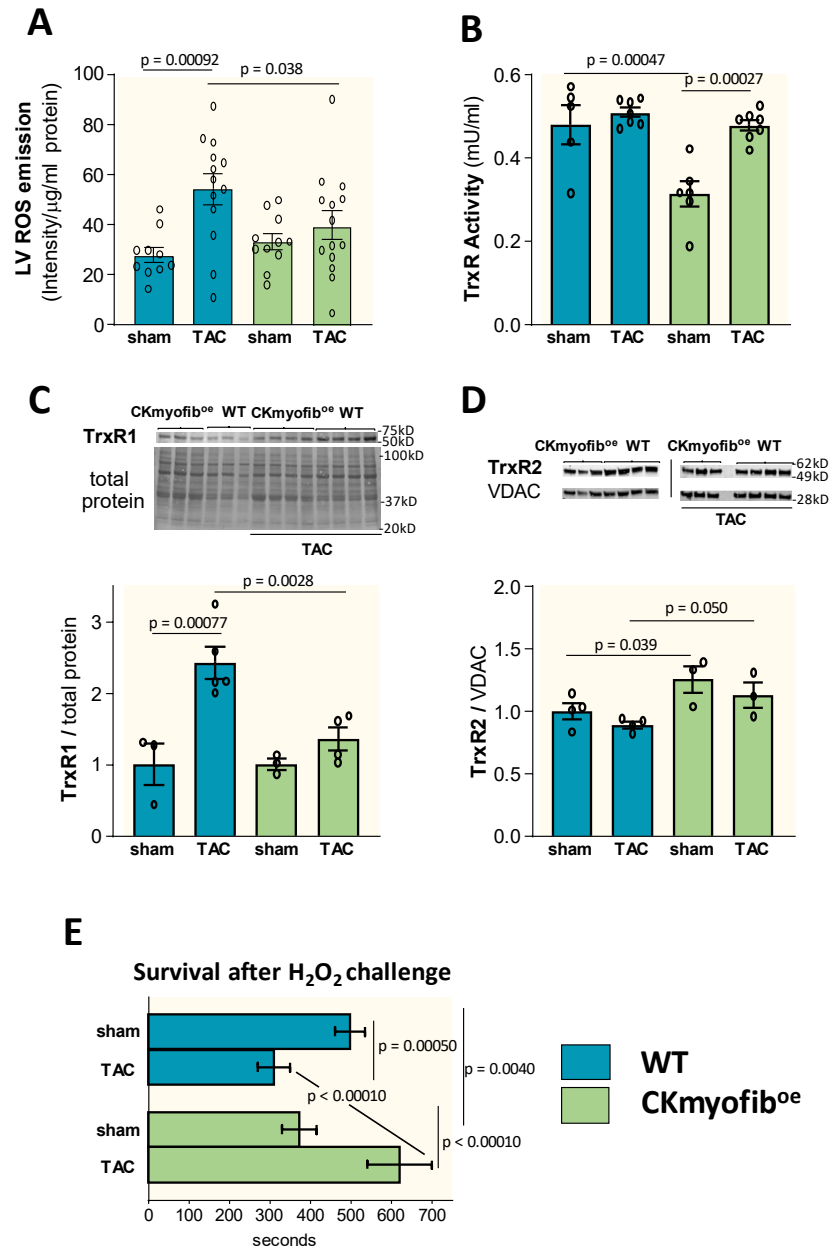


Figure S5. Effect of myofibrillar creatine kinase (CKmyofib) overexpression on reactive oxygen species (ROS) levels and antioxidant enzymes during TAC heart failure. (A) ROS production measured by electron paramagnetic resonance (EPR) spectroscopy in left ventricles (LVs) of WT or cardiac-specific CKmyofib overexpressing (CKmyofib^{oe}) sham or TAC hearts (experimental replicates: n=10 (WT sham), n=13 (WT TAC), n=11 (CKmyofib^{oe} sham), and n=14 (CKmyofib^{oe} TAC)). LVs from WT or CKmyofib^{oe} hearts were isolated and analyzed. **(B)** Thioredoxin reductase (TrxR) activities determined

in sham or TAC heart homogenates in the presence of excess NADPH (experimental replicates: n=5 (WT sham), n=7 (WT TAC or CKmyofib^{oe} TAC), and n=6 (CKmyofib^{oe} sham)). Representative immunoblots and summary of data showing expression levels of **(C)** TrxR1 and **(D)** TrxR2 normalized to total protein **(C)** or VDAC (voltage-dependent anion channel) **(D)** and presented as relative to the amount of protein detected in sham WT hearts (experimental replicates: n=3 (WT sham or CKmyofib^{oe} sham), n=5 (WT TAC), and n=4 (CKmyofib^{oe} TAC) **(C)**; n=4 (WT sham or WT TAC) and n=3 (CKmyofib^{oe} sham or CKmyofib^{oe} TAC) **(D)**). **(E)** Cardiomyocytes isolated from WT[±] or CKmyofib^{oe} sham or TAC hearts were exposed to H₂O₂ (50 μM) for 700 s, and time to irreversible arrhythmia/cell death was monitored (experimental replicates: n=20 cells isolated from 6 mice (WT sham), n=6 cells isolated from 2 mice (WT TAC), n=17 cells isolated from 4 mice (CKmyofib^{oe} sham), and n=7 cells isolated from 2 mice (CKmyofib^{oe} TAC)). (±Same WT cardiomyocytes were employed for Figs 3C and Supplemental Fig 5E since the experiments were conducted on the same day and under the same experimental conditions.) Graphs show data points for individual mice **(A-D)**. Data were tested for normality using the Kolmogorov-Smirnov test for normality and analyzed by two-way ANOVA followed by Tukey's post-hoc multiple comparison test **(A-D)**, while a generalized estimating equation model was used to take into account the correlation of within-subject data **(E)**. The error bars represent ±SEM.

Online Table I. Statistical Analyses						
Figure ID	Normality	(Non-) Parametric testing	Post-hoc multiple comparisons testing	Comparison (n1 vs. n2)	Summary	P value
Fig. 1A	Yes	two-tailed Student's <i>t</i> -test	N/A	healthy controls vs. heart failure patients (14 vs. 27)	****	0.000043
Fig. 1B	Yes	two-tailed Student's <i>t</i> -test	N/A	healthy controls vs. heart failure patients (14 vs. 27)	****	0.000066
Fig. 1C	Yes	two-tailed Student's <i>t</i> -test	N/A	healthy controls vs. heart failure patients (14 vs. 27)	**	≤ 0.0020
Fig. 1D	Yes	two-tailed Student's <i>t</i> -test	N/A	healthy controls vs. heart failure patients (14 vs. 27)	**	0.010
Fig. 1E	Yes	linear regression model	N/A	N/A	*	0.033
Fig. 1F	Yes	linear regression model	N/A	N/A	**	0.0084
Fig. 1G	Yes	linear regression model	N/A	N/A	**	0.0067
Fig. 1H	Yes	linear regression model	N/A	N/A	**	0.0022
Fig. 2A	Yes	two-tailed Student's <i>t</i> -test	N/A	WT LV vs. CKmito ^{oe} LV (4 vs. 5)	***	0.00090
	Yes	two-tailed Student's <i>t</i> -test	N/A	WT Atria vs. CKmito ^{oe} Atria (4 vs. 5)	**	0.0044
Fig. 2A (non-parametric alternative)		Wilcoxon signed rank test	N/A	WT LV vs. CKmito ^{oe} LV (4 vs. 5)	***	0.024
		Wilcoxon signed rank test	N/A	WT Atria vs. CKmito ^{oe} Atria (4 vs. 5)	**	0.024
Fig. 2F	Yes	two-way ANOVA	Tukey's multiple comparisons test	WT sham vs. WT TAC (5 vs. 8)	***	0.00015
				CKmito ^{oe} sham vs. CKmito ^{oe} TAC (8 vs. 7)	**	0.0044
				WT sham vs. CKmito ^{oe} sham (5 vs. 8)	ns	0.155
				WT TAC vs. CKmito ^{oe} TAC (8 vs. 7)	*	0.045
Fig. 2F (non-parametric alternative)		Wilcoxon signed rank test	pairwise, two-sided multiple comparison analysis (Dwass, Steel, Crichlow-Fligner Method)	WT sham vs. WT TAC (5 vs. 8)	*	0.018
				CKmito ^{oe} sham vs. CKmito ^{oe} TAC (8 vs. 7)	ns	0.094
				WT sham vs. CKmito ^{oe} sham (5 vs. 8)	ns	0.458
				WT TAC vs. CKmito ^{oe} TAC (8 vs. 7)	ns	0.435
Fig. 2G	Yes	two-way ANOVA	Tukey's multiple comparisons test	WT sham vs. WT TAC (5 vs. 8)	***	0.00015
				CKmito ^{oe} sham vs. CKmito ^{oe} TAC (8 vs. 7)	***	0.00015
				WT sham vs. CKmito ^{oe} sham (5 vs. 8)	ns	0.268
				WT TAC vs. CKmito ^{oe} TAC (8 vs. 7)	*	0.027

Fig. 2G (non-parametric alternative)		Wilcoxon signed rank test	pairwise, two-sided multiple comparison analysis (Dwass, Steel, Crichlow-Fligner Method)	WT sham vs. WT TAC (5 vs. 8)	*	0.018
				CKmito ^{oe} sham vs. CKmito ^{oe} TAC (8 vs. 7)	**	0.0065
				WT sham vs. CKmito ^{oe} sham (5 vs. 8)	ns	0.645
				WT TAC vs. CKmito ^{oe} TAC (8 vs. 7)	ns	0.434
Fig. 2H	Yes	two-way ANOVA	Tukey's multiple comparisons test	WT sham vs. WT TAC (5 vs. 8)	***	0.00015
				CKmito ^{oe} sham vs. CKmito ^{oe} TAC (8 vs. 7)	***	0.00043
				WT sham vs. CKmito ^{oe} sham (5 vs. 8)	***	0.00015
				WT TAC vs. CKmito ^{oe} TAC (8 vs. 7)	***	0.00015
Fig. 2H (non-parametric alternative)		Wilcoxon signed rank test	pairwise, two-sided multiple comparison analysis (Dwass, Steel, Crichlow-Fligner Method)	WT sham vs. WT TAC (5 vs. 8)	*	0.018
				CKmito ^{oe} sham vs. CKmito ^{oe} TAC (8 vs. 7)	*	0.028
				WT sham vs. CKmito ^{oe} sham (5 vs. 8)	*	0.018
				WT TAC vs. CKmito ^{oe} TAC (8 vs. 7)	**	0.0064
Fig. 2I	Yes	two-way ANOVA	Tukey's multiple comparisons test	WT sham vs. WT TAC (5 vs. 8)	***	0.00015
				CKmito ^{oe} sham vs. CKmito ^{oe} TAC (8 vs. 7)	***	0.00015
				WT sham vs. CKmito ^{oe} sham (5 vs. 8)	***	0.00023
				WT TAC vs. CKmito ^{oe} TAC (8 vs. 7)	***	0.00015
Fig. 2I (non-parametric alternative)		Wilcoxon signed rank test	pairwise, two-sided multiple comparison analysis (Dwass, Steel, Crichlow-Fligner Method)	WT sham vs. WT TAC (5 vs. 8)	*	0.018
				CKmito ^{oe} sham vs. CKmito ^{oe} TAC (8 vs. 7)	**	0.0066
				WT sham vs. CKmito ^{oe} sham (5 vs. 8)	*	0.018
				WT TAC vs. CKmito ^{oe} TAC (8 vs. 7)	**	0.0065
Fig. 2J	Yes	two-way ANOVA	Tukey's multiple comparisons test	WT sham vs. WT TAC (5 vs. 12)	***	0.00014
				CKmito ^{oe} sham vs. CKmito ^{oe} TAC (8 vs. 7)	***	0.00014
				WT sham vs. CKmito ^{oe} sham (5 vs. 8)	ns	0.746
				WT TAC vs. CKmito ^{oe} TAC (12 vs. 7)	***	0.00014
Fig. 2J (non-parametric alternative)		Wilcoxon signed rank test	pairwise, two-sided multiple comparison analysis (Dwass, Steel, Crichlow-Fligner Method)	WT sham vs. WT TAC (5 vs. 12)	**	0.0085
				CKmito ^{oe} sham vs. CKmito ^{oe} TAC (8 vs. 7)	**	0.0066
				WT sham vs. CKmito ^{oe} sham (5 vs. 8)	ns	0.645
				WT TAC vs. CKmito ^{oe} TAC (12 vs. 7)	**	0.0022

Fig. 2K	Yes	two-way ANOVA	Tukey's multiple comparisons test	WT sham vs. WT TAC (5 vs. 12)	***	0.00014
				CKmito ^{oe} sham vs. CKmito ^{oe} TAC (8 vs. 7)	ns	0.073
				WT sham vs. CKmito ^{oe} sham (5 vs. 8)	ns	0.330
				WT TAC vs. CKmito ^{oe} TAC (12 vs. 7)	***	0.00014
Fig. 2K (non-parametric alternative)		Wilcoxon signed rank test	pairwise, two-sided multiple comparison analysis (Dwass, Steel, Crichlow-Fligner Method)	WT sham vs. WT TAC (5 vs. 12)	**	0.0085
				CKmito ^{oe} sham vs. CKmito ^{oe} TAC (8 vs. 7)	ns	0.072
				WT sham vs. CKmito ^{oe} sham (5 vs. 8)	ns	0.884
				WT TAC vs. CKmito ^{oe} TAC (12 vs. 7)	**	0.0022
Fig. 2L	No	Wilcoxon signed rank test	pairwise, two-sided multiple comparison analysis (Dwass, Steel, Crichlow-Fligner Method)	WT sham vs. WT TAC (5 vs. 12)	**	0.0085
				CKmito ^{oe} sham vs. CKmito ^{oe} TAC (8 vs. 7)	**	0.0066
				WT sham vs. CKmito ^{oe} sham (5 vs. 8)	ns	0.972
				WT TAC vs. CKmito ^{oe} TAC (12 vs. 7)	**	0.0022
Fig. 2M	Yes	two-way ANOVA	Tukey's multiple comparisons test	WT sham vs. WT TAC (5 vs. 12)	***	0.00014
				CKmito ^{oe} sham vs. CKmito ^{oe} TAC (8 vs. 7)	***	0.00014
				WT sham vs. CKmito ^{oe} sham (5 vs. 8)	ns	0.607
				WT TAC vs. CKmito ^{oe} TAC (12 vs. 7)	***	0.00017
Fig. 2M (non-parametric alternative)		Wilcoxon signed rank test	pairwise, two-sided multiple comparison analysis (Dwass, Steel, Crichlow-Fligner Method)	WT sham vs. WT TAC (5 vs. 12)	**	0.0085
				CKmito ^{oe} sham vs. CKmito ^{oe} TAC (8 vs. 7)	**	0.0065
				WT sham vs. CKmito ^{oe} sham (5 vs. 8)	ns	0.936
				WT TAC vs. CKmito ^{oe} TAC (12 vs. 7)	**	0.0047
Fig. 2N	No	Wilcoxon signed rank test	pairwise, two-sided multiple comparison analysis (Dwass, Steel, Crichlow-Fligner Method)	WT sham vs. WT TAC (6 vs. 9)	**	0.0080
				CKmyofib ^{oe} sham vs. CKmyofib ^{oe} TAC (6 vs. 7)	*	0.014
				WT sham vs. CKmyofib ^{oe} sham (6 vs. 6)	ns	0.989
				WT TAC vs. CKmyofib ^{oe} TAC (9 vs. 7)	ns	0.548
Fig. 2O	Yes	two-way ANOVA	Tukey's multiple comparisons test	WT sham vs. WT TAC (6 vs. 9)	***	0.00026
				CKmyofib ^{oe} sham vs. CKmyofib ^{oe} TAC (6 vs. 7)	***	0.013
				WT sham vs. CKmyofib ^{oe} sham (6 vs. 6)	ns	0.783
				WT TAC vs. CKmyofib ^{oe} TAC (9 vs. 7)	ns	0.142

Fig. 2P	Yes	two-way ANOVA	Tukey's multiple comparisons test	WT saline vs. WT ISO (5 vs. 7)	***	0.00015
				CKmito ^{oe} saline vs. CKmito ^{oe} ISO (5 vs. 10)	***	0.00030
				WT saline vs. CKmito ^{oe} saline (5 vs. 5)	ns	0.608
				WT ISO vs. CKmito ^{oe} ISO (7 vs. 10)	***	0.00019
Fig. 2P (non-parametric alternative)		Wilcoxon signed rank test	pairwise, two-sided multiple comparison analysis (Dwass, Steel, Crichlow-Fligner Method)	WT saline vs. WT ISO (5 vs. 7)	*	0.023
				CKmito ^{oe} saline vs. CKmito ^{oe} ISO (5 vs. 10)	*	0.012
				WT saline vs. CKmito ^{oe} saline (5 vs. 5)	ns	0.659
				WT ISO vs. CKmito ^{oe} ISO (7 vs. 10)	**	0.0097
Fig. 2Q	Yes	two-way ANOVA	Tukey's multiple comparisons test	WT saline vs. WT ISO (5 vs. 7)	ns	0.351
				CKmito ^{oe} saline vs. CKmito ^{oe} ISO (5 vs. 10)	ns	0.329
				WT saline vs. CKmito ^{oe} saline (5 vs. 5)	*	0.013
				WT ISO vs. CKmito ^{oe} ISO (7 vs. 10)	ns	0.239
Fig. 2Q (non-parametric alternative)		Wilcoxon signed rank test	pairwise, two-sided multiple comparison analysis (Dwass, Steel, Crichlow-Fligner Method)	WT saline vs. WT ISO (5 vs. 7)	ns	0.808
				CKmito ^{oe} saline vs. CKmito ^{oe} ISO (5 vs. 10)	ns	0.827
				WT saline vs. CKmito ^{oe} saline (5 vs. 5)	*	0.045
				WT ISO vs. CKmito ^{oe} ISO (7 vs. 10)	ns	0.763
Fig. 3B	Yes	two-way ANOVA	Tukey's multiple comparisons test	WT sham vs. WT TAC (10 vs. 13)	**	0.0035
				CKmito ^{oe} sham vs. CKmito ^{oe} TAC (10 vs. 13)	ns	0.203
				WT sham vs. CKmito ^{oe} sham (10 vs. 10)	ns	0.526
				WT TAC vs. CKmito ^{oe} TAC (13 vs. 13)	ns	0.229
Fig. 3C		generalized estimating equation model to take into account the correlation of within-subject data		WT sham vs. WT TAC (20 cells (from 6 mice) vs. 6 cells (from 2 mice))	***	0.00050
				CKmito ^{oe} sham vs. CKmito ^{oe} TAC (20 cells (from 5 mice) vs. 10 cells (from 4 mice))	ns	0.146
				WT sham vs. CKmito ^{oe} sham (20 cells (from 6 mice) vs. 20 cells (from 5 mice))	*	0.014
				WT TAC vs. CKmito ^{oe} TAC (6 cells (from 2 mice) vs. 10 cells (from 4 mice))	ns	0.069
Fig. 3D	Yes	two-way ANOVA	Tukey's multiple comparisons test	WT sham vs. WT TAC (5 vs. 7)	ns	0.528
				CKmito ^{oe} sham vs. CKmito ^{oe} TAC (4 vs. 7)	***	0.00064
				WT sham vs. CKmito ^{oe} sham (5 vs. 4)	ns	0.298
				WT TAC vs. CKmito ^{oe} TAC (7 vs. 7)	**	0.010

Fig. 3D (non-parametric alternative)		Kruskal-Wallis test	pair-wise, two-sided multiple comparison analysis (Dunn method with Benjamini-Hochberg adjustment for multiple comparisons)	WT sham vs. WT TAC (5 vs. 7)	ns	0.954
				CKmito ^{oe} sham vs. CKmito ^{oe} TAC (4 vs. 7)	*	0.018
				WT sham vs. CKmito ^{oe} sham (5 vs. 4)	ns	0.702
				WT TAC vs. CKmito ^{oe} TAC (7 vs. 7)	*	0.025
Fig. 3E	Yes	two-way ANOVA	Tukey's multiple comparisons test	WT sham vs. WT TAC (3 vs. 5)	**	0.0028
				CKmito ^{oe} sham vs. CKmito ^{oe} TAC (5 vs. 5)	ns	0.119
				WT sham vs. CKmito ^{oe} sham (3 vs. 5)	*	0.044
				WT TAC vs. CKmito ^{oe} TAC (5 vs. 5)	ns	1.00
Fig. 3E (non-parametric alternative)		Kruskal-Wallis test	pair-wise, two-sided multiple comparison analysis (Dunn method with Benjamini-Hochberg adjustment for multiple comparisons)	WT sham vs. WT TAC (3 vs. 5)	*	0.012
				CKmito ^{oe} sham vs. CKmito ^{oe} TAC (5 vs. 5)	ns	0.515
				WT sham vs. CKmito ^{oe} sham (3 vs. 5)	ns	0.082
				WT TAC vs. CKmito ^{oe} TAC (5 vs. 5)		0.194
Fig. 3F	Yes	two-way ANOVA	Tukey's multiple comparisons test	WT sham vs. WT TAC (4 vs. 4)	ns	0.274
				CKmito ^{oe} sham vs. CKmito ^{oe} TAC (4 vs. 4)	ns	0.125
				WT sham vs. CKmito ^{oe} sham (4 vs. 4)	ns	0.947
				WT TAC vs. CKmito ^{oe} TAC (4 vs. 4)	*	0.019
Fig. 3F (non-parametric alternative)		Kruskal-Wallis test	pair-wise, two-sided multiple comparison analysis (Dunn method with Benjamini-Hochberg adjustment for multiple comparisons)	WT sham vs. WT TAC (4 vs. 4)	ns	0.544
				CKmito ^{oe} sham vs. CKmito ^{oe} TAC (4 vs. 4)	ns	0.47
				WT sham vs. CKmito ^{oe} sham (4 vs. 4)	ns	0.824
				WT TAC vs. CKmito ^{oe} TAC (4 vs. 4)	ns	0.128
Fig. 3G	Yes	two-way ANOVA	Tukey's multiple comparisons test	WT sham vs. WT TAC (9 vs. 8)	ns	0.070
				CKmito ^{oe} sham vs. CKmito ^{oe} TAC (9 vs. 9)	ns	0.599
				WT sham vs. CKmito ^{oe} sham (9 vs. 9)	**	0.0030
				WT TAC vs. CKmito ^{oe} TAC (8 vs. 9)	ns	0.457
Fig. 3H	Yes	two-way ANOVA	Tukey's multiple comparisons test	WT sham vs. WT TAC (7 vs. 7)	ns	0.800
				CKmito ^{oe} sham vs. CKmito ^{oe} TAC (6 vs. 7)	***	0.00075
				WT sham vs. CKmito ^{oe} sham (7 vs. 6)	**	0.0046
				WT TAC vs. CKmito ^{oe} TAC (7 vs. 7)	ns	0.282

Fig. 4A	Yes	two-tailed Student's <i>t</i> -test	N/A	WT sham vs. CKmito ^{oe} sham (4 vs. 4)	ns	0.329
Fig. 4A (non-parametric alternative)		Wilcoxon signed rank test	N/A	WT sham vs. CKmito ^{oe} sham (4 vs. 4)	ns	0.329
Fig. 4B		generalized estimating equation model to take into account the correlation of within-subject data		WT sham vs. WT TAC (12 cells (from 3 mice) vs. 7 cells (from 2 mice))	****	< 0.00010
				CKmito ^{oe} sham vs. CKmito ^{oe} TAC (6 cells (from 2 mice) vs. 10 cells (from 6 mice))	ns	0.627
				WT sham vs. CKmito ^{oe} sham (12 cells (from 3 mice) vs. 6 cells (from 2 mice))	ns	0.611
				WT TAC vs. CKmito ^{oe} TAC (7 cells (from 2 mice) vs. 10 cells (from 6 mice))	ns	0.070
Fig. 4C		generalized estimating equation model to take into account the correlation of within-subject data		WT sham vs. WT TAC (11 cells (from 3 mice) vs. 7 cells (from 2 mice))	****	< 0.00010
				CKmito ^{oe} sham vs. CKmito ^{oe} TAC (6 cells (from 2 mice) vs. 6 cells (from 2 mice))	ns	0.872
				WT sham vs. CKmito ^{oe} sham (11 cells (from 3 mice) vs. 6 cells (from 2 mice))	****	< 0.00010
				WT TAC vs. CKmito ^{oe} TAC (7 cells (from 2 mice) vs. 6 cells (from 2 mice))	ns	0.130
Fig. 4D	Yes	two-way ANOVA	Tukey's multiple comparisons test	WT sham vs. WT TAC (6 vs. 5)	ns	
				CKmito ^{oe} sham vs. CKmito ^{oe} TAC (3 vs. 4)	ns	
				WT sham vs. CKmito ^{oe} sham (6 vs. 3)	ns	
				WT TAC vs. CKmito ^{oe} TAC (5 vs. 4)	ns	
Fig. 4D (non-parametric alternative)		Kruskal-Wallis test	pair-wise, two-sided multiple comparison analysis (Dunn method with Benjamini-Hochberg adjustment for multiple comparisons)	WT sham vs. WT TAC (6 vs. 5)	Ns	0.251
				CKmito ^{oe} sham vs. CKmito ^{oe} TAC (3 vs. 4)	Ns	0.236
				WT sham vs. CKmito ^{oe} sham (6 vs. 3)	Ns	0.363
				WT TAC vs. CKmito ^{oe} TAC (5 vs. 4)	ns	0.539
Fig. 4E	Yes	two-way ANOVA	Tukey's multiple comparisons test	WT sham vs. WT TAC (6 vs. 5)	***	0.00019
				CKmito ^{oe} sham vs. CKmito ^{oe} TAC (3 vs. 4)	ns	0.059
				WT sham vs. CKmito ^{oe} sham (6 vs. 3)	ns	0.339
				WT TAC vs. CKmito ^{oe} TAC (5 vs. 4)	*	0.029
Fig. 4E (non-parametric alternative)		Kruskal-Wallis test	pair-wise, two-sided multiple comparison analysis (Dunn method with	WT sham vs. WT TAC (6 vs. 5)	**	0.0028
				CKmito ^{oe} sham vs. CKmito ^{oe} TAC (3 vs. 4)	ns	0.238

			Benjamini-Hochberg adjustment for multiple comparisons)	WT sham vs. CKmito ^{oe} sham (6 vs. 3)	ns	0.691
				WT TAC vs. CKmito ^{oe} TAC (5 vs. 4)	ns	0.31
Fig. 4F	Yes	two-way ANOVA	Tukey's multiple comparisons test	WT sham vs. WT TAC (6 vs. 5)	ns	
				CKmito ^{oe} sham vs. CKmito ^{oe} TAC (3 vs. 4)	ns	
				WT sham vs. CKmito ^{oe} sham (6 vs. 3)	ns	
				WT TAC vs. CKmito ^{oe} TAC (5 vs. 4)	ns	
Fig. 4F (non-parametric alternative)		Kruskal-Wallis test	pair-wise, two-sided multiple comparison analysis (Dunn method with Benjamini-Hochberg adjustment for multiple comparisons)	WT sham vs. WT TAC (6 vs. 5)	ns	0.942
				CKmito ^{oe} sham vs. CKmito ^{oe} TAC (3 vs. 4)	ns	0.191
				WT sham vs. CKmito ^{oe} sham (6 vs. 3)	ns	0.163
				WT TAC vs. CKmito ^{oe} TAC (5 vs. 4)	ns	0.994
Fig. 4G	Yes	two-way ANOVA	Tukey's multiple comparisons test	WT sham vs. WT TAC (6 vs. 5)	***	0.00044
				CKmito ^{oe} sham vs. CKmito ^{oe} TAC (3 vs. 4)	ns	0.065
				WT sham vs. CKmito ^{oe} sham (6 vs. 3)	ns	0.234
				WT TAC vs. CKmito ^{oe} TAC (5 vs. 4)	***	0.00027
Fig. 4G (non-parametric alternative)		Kruskal-Wallis test	pair-wise, two-sided multiple comparison analysis (Dunn method with Benjamini-Hochberg adjustment for multiple comparisons)	WT sham vs. WT TAC (6 vs. 5)	*	0.0244
				CKmito ^{oe} sham vs. CKmito ^{oe} TAC (3 vs. 4)	ns	0.217
				WT sham vs. CKmito ^{oe} sham (6 vs. 3)	ns	0.365
				WT TAC vs. CKmito ^{oe} TAC (5 vs. 4)	**	0.0066
Fig. 4H	Yes	two-way ANOVA	Tukey's multiple comparisons test	WT sham vs. WT TAC (6 vs. 5)	ns	
				CKmito ^{oe} sham vs. CKmito ^{oe} TAC (2 vs. 4)	ns	
				WT sham vs. CKmito ^{oe} sham (6 vs. 2)	ns	
				WT TAC vs. CKmito ^{oe} TAC (5 vs. 4)	ns	
Fig. 4H (non-parametric alternative)		Kruskal-Wallis test	pair-wise, two-sided multiple comparison analysis (Dunn method with Benjamini-Hochberg adjustment for multiple comparisons)	WT sham vs. WT TAC (6 vs. 5)	ns	0.842
				CKmito ^{oe} sham vs. CKmito ^{oe} TAC (2 vs. 4)	ns	1.0
				WT sham vs. CKmito ^{oe} sham (6 vs. 2)	ns	0.816
				WT TAC vs. CKmito ^{oe} TAC (5 vs. 4)	ns	0.678

Fig. 4I	Yes	two-way ANOVA	Tukey's multiple comparisons test	WT sham vs. WT TAC (6 vs. 5)	*	0.013
				CKmito ^{oe} sham vs. CKmito ^{oe} TAC (3 vs. 4)	ns	0.237
				WT sham vs. CKmito ^{oe} sham (6 vs. 3)	***	0.00024
				WT TAC vs. CKmito ^{oe} TAC (5 vs. 4)	***	0.00018
Fig. 4I (non-parametric alternative)		Kruskal-Wallis test	pair-wise, two-sided multiple comparison analysis (Dunn method with Benjamini-Hochberg adjustment for multiple comparisons)	WT sham vs. WT TAC (6 vs. 5)	ns	0.368
				CKmito ^{oe} sham vs. CKmito ^{oe} TAC (3 vs. 4)	ns	0.431
				WT sham vs. CKmito ^{oe} sham (6 vs. 3)	ns	0.199
				WT TAC vs. CKmito ^{oe} TAC (5 vs. 4)	ns	0.0040
Fig. 4J	Yes	two-way ANOVA	Tukey's multiple comparisons test	WT sham vs. WT TAC (3 vs. 3)	ns	
				CKmito ^{oe} sham vs. CKmito ^{oe} TAC (3 vs. 3)	ns	
				WT sham vs. CKmito ^{oe} sham (3 vs. 3)	ns	
				WT TAC vs. CKmito ^{oe} TAC (3 vs. 3)	ns	
Fig. 4J (non-parametric alternative)		Kruskal-Wallis test	pair-wise, two-sided multiple comparison analysis (Dunn method with Benjamini-Hochberg adjustment for multiple comparisons)	WT sham vs. WT TAC (3 vs. 3)	ns	1.00
				CKmito ^{oe} sham vs. CKmito ^{oe} TAC (3 vs. 3)	ns	0.730
				WT sham vs. CKmito ^{oe} sham (6 vs. 3)	ns	1.00
				WT TAC vs. CKmito ^{oe} TAC (5 vs. 4)	ns	0.642
Fig. 4K	Yes	two-way ANOVA	Tukey's multiple comparisons test	WT sham vs. WT TAC (3 vs. 5)	***	0.00018
				CKmito ^{oe} sham vs. CKmito ^{oe} TAC (4 vs. 5)	***	0.00021
				WT sham vs. CKmito ^{oe} sham (3 vs. 4)	*	0.022
				WT TAC vs. CKmito ^{oe} TAC (5 vs. 5)	ns	0.154
Fig. 4K (non-parametric alternative)		Kruskal-Wallis test	pair-wise, two-sided multiple comparison analysis (Dunn method with Benjamini-Hochberg adjustment for multiple comparisons)	WT sham vs. WT TAC (3 vs. 5)	**	0.010
				CKmito ^{oe} sham vs. CKmito ^{oe} TAC (4 vs. 5)	ns	0.126
				WT sham vs. CKmito ^{oe} sham (3 vs. 4)	ns	0.449
				WT TAC vs. CKmito ^{oe} TAC (5 vs. 5)	ns	0.456
Fig. 4L	Yes	two-way ANOVA	Tukey's multiple comparisons test	WT sham vs. WT TAC (3 vs. 2)	***	0.00048
				CKmito ^{oe} sham vs. CKmito ^{oe} TAC (3 vs. 2)	***	0.00023
				WT sham vs. CKmito ^{oe} sham (3 vs. 3)	***	0.00024
				WT TAC vs. CKmito ^{oe} TAC (2 vs. 2)	ns	0.109

Fig. 4L (non-parametric alternative)		Kruskal-Wallis test	pair-wise, two-sided multiple comparison analysis (Dunn method with Benjamini-Hochberg adjustment for multiple comparisons)	WT sham vs. WT TAC (3 vs. 2)	ns	0.207
				CKmito ^{oe} sham vs. CKmito ^{oe} TAC (3 vs. 2)	ns	0.14
				WT sham vs. CKmito ^{oe} sham (3 vs. 3)	ns	0.337
				WT TAC vs. CKmito ^{oe} TAC (2 vs. 2)	ns	0.509
Fig. 5A	No	Kruskal-Wallis test	pair-wise, two-sided multiple comparison analysis (Dunn method with Benjamini-Hochberg adjustment for multiple comparisons)	GAMT ^{-/-} x WT sham vs. GAMT ^{-/-} x WT TAC (5 vs. 12)	**	0.0020
				GAMT ^{-/-} x CKmito ^{oe} sham vs. GAMT ^{-/-} x CKmito ^{oe} TAC (5 vs. 8)	*	0.015
				GAMT ^{-/-} x WT sham vs. GAMT ^{-/-} x CKmito ^{oe} sham (5 vs. 5)	ns	0.858
				GAMT ^{-/-} x WT TAC vs. GAMT ^{-/-} x CKmito ^{oe} TAC (5 vs. 8)	ns	0.454
Fig. 5B	Yes	two-way ANOVA	Tukey's multiple comparisons test	GAMT ^{-/-} x WT sham vs. GAMT ^{-/-} x WT TAC (5 vs. 12)	***	0.00017
				GAMT ^{-/-} x CKmito ^{oe} sham vs. GAMT ^{-/-} x CKmito ^{oe} TAC (5 vs. 8)	**	0.010
				GAMT ^{-/-} x WT sham vs. GAMT ^{-/-} x CKmito ^{oe} sham (5 vs. 5)	ns	0.361
				GAMT ^{-/-} x WT TAC vs. GAMT ^{-/-} x CKmito ^{oe} TAC (5 vs. 8)	ns	0.238
Fig. 5B (non-parametric alternative)		Kruskal-Wallis test	pair-wise, two-sided multiple comparison analysis (Dunn method with Benjamini-Hochberg adjustment for multiple comparisons)	GAMT ^{-/-} x WT sham vs. GAMT ^{-/-} x WT TAC (5 vs. 12)	**	0.0017
				GAMT ^{-/-} x CKmito ^{oe} sham vs. GAMT ^{-/-} x CKmito ^{oe} TAC (5 vs. 8)	*	0.028
				GAMT ^{-/-} x WT sham vs. GAMT ^{-/-} x CKmito ^{oe} sham (5 vs. 5)	ns	0.621
				GAMT ^{-/-} x WT TAC vs. GAMT ^{-/-} x CKmito ^{oe} TAC (5 vs. 8)	ns	0.686
Fig. 5C	Yes	two-way ANOVA	Tukey's multiple comparisons test	GAMT ^{-/-} x WT sham vs. GAMT ^{-/-} x WT TAC (5 vs. 8)	ns	0.170
				GAMT ^{-/-} x CKmito ^{oe} sham vs. GAMT ^{-/-} x CKmito ^{oe} TAC (5 vs. 5)	ns	0.056
				GAMT ^{-/-} x WT sham vs. GAMT ^{-/-} x CKmito ^{oe} sham (5 vs. 5)	ns	0.676
				GAMT ^{-/-} x WT TAC vs. GAMT ^{-/-} x CKmito ^{oe} TAC (8 vs. 5)	ns	0.721

Fig. 5C (non-parametric alternative)		Kruskal-Wallis test	pair-wise, two-sided multiple comparison analysis (Dunn method with Benjamini-Hochberg adjustment for multiple comparisons)	GAMT ^{-/-} x WT sham vs. GAMT ^{-/-} x WT TAC (5 vs. 8)	ns	0.186
				GAMT ^{-/-} x CKmito ^{oe} sham vs. GAMT ^{-/-} x CKmito ^{oe} TAC (5 vs. 5)	ns	0.168
				GAMT ^{-/-} x WT sham vs. GAMT ^{-/-} x CKmito ^{oe} sham (5 vs. 5)	ns	0.691
				GAMT ^{-/-} x WT TAC vs. GAMT ^{-/-} x CKmito ^{oe} TAC (8 vs. 5)	ns	0.856
Fig. 5D		generalized estimating equation model to take into account the correlation of within-subject data		GAMT ^{-/-} x WT sham vs. GAMT ^{-/-} x WT TAC (19 cells (from 3 mice) vs. 12 cells (from 2 mice))	ns	0.499
				GAMT ^{-/-} x CKmito ^{oe} sham vs. GAMT ^{-/-} x CKmito ^{oe} TAC (18 cells (from 3 mice) vs. 12 cells (from 2 mice))	ns	0.146
				GAMT ^{-/-} x WT sham vs. GAMT ^{-/-} x CKmito ^{oe} sham (19 cells (from 3 mice) vs. 18 cells (from 3 mice))	*	0.044
				GAMT ^{-/-} x WT TAC vs. GAMT ^{-/-} x CKmito ^{oe} TAC (12 cells (from 2 mice) vs. 12 cells (from 2 mice))	ns	0.674
Fig. 5E	Yes	two-way ANOVA	Tukey's multiple comparisons test	GAMT ^{-/-} x WT sham vs. GAMT ^{-/-} x WT TAC (5 vs. 7)	ns	0.093
				GAMT ^{-/-} x CKmito ^{oe} sham vs. GAMT ^{-/-} x CKmito ^{oe} TAC (5 vs. 5)	ns	0.861
				GAMT ^{-/-} x WT sham vs. GAMT ^{-/-} x CKmito ^{oe} sham (5 vs. 5)	ns	0.761
				GAMT ^{-/-} x WT TAC vs. GAMT ^{-/-} x CKmito ^{oe} TAC (7 vs. 5)	ns	0.120
Fig. 5E (non-parametric alternative)		Kruskal-Wallis test	pair-wise, two-sided multiple comparison analysis (Dunn method with Benjamini-Hochberg adjustment for multiple comparisons)	GAMT ^{-/-} x WT sham vs. GAMT ^{-/-} x WT TAC (5 vs. 7)	ns	0.444
				GAMT ^{-/-} x CKmito ^{oe} sham vs. GAMT ^{-/-} x CKmito ^{oe} TAC (5 vs. 5)	ns	0.728
				GAMT ^{-/-} x WT sham vs. GAMT ^{-/-} x CKmito ^{oe} sham (5 vs. 5)	ns	0.275
				GAMT ^{-/-} x WT TAC vs. GAMT ^{-/-} x CKmito ^{oe} TAC (7 vs. 5)	ns	0.880

Fig. 5F	Yes	two-way ANOVA	Tukey's multiple comparisons test	GAMT ^{-/-} x WT sham vs. GAMT ^{-/-} x WT TAC (5 vs. 7)	ns	0.276
				GAMT ^{-/-} x CKmito ^{oe} sham vs. GAMT ^{-/-} x CKmito ^{oe} TAC (5 vs. 5)	ns	0.236
				GAMT ^{-/-} x WT sham vs. GAMT ^{-/-} x CKmito ^{oe} sham (5 vs. 5)	*	0.045
				GAMT ^{-/-} x WT TAC vs. GAMT ^{-/-} x CKmito ^{oe} TAC (7 vs. 5)	ns	0.909
Fig. 5F (non-parametric alternative)		Kruskal-Wallis test	pair-wise, two-sided multiple comparison analysis (Dunn method with Benjamini-Hochberg adjustment for multiple comparisons)	GAMT ^{-/-} x WT sham vs. GAMT ^{-/-} x WT TAC (5 vs. 7)	ns	1.0
				GAMT ^{-/-} x CKmito ^{oe} sham vs. GAMT ^{-/-} x CKmito ^{oe} TAC (5 vs. 5)	ns	0.836
				GAMT ^{-/-} x WT sham vs. GAMT ^{-/-} x CKmito ^{oe} sham (5 vs. 5)	ns	1.0
				GAMT ^{-/-} x WT TAC vs. GAMT ^{-/-} x CKmito ^{oe} TAC (7 vs. 5)	ns	1.0
Fig. 6A	No	Kruskal-Wallis test	pair-wise, two-sided multiple comparison analysis (Dunn method with Benjamini-Hochberg adjustment for multiple comparisons)	WT sham vs. WT TAC (10 vs. 10)	*	0.019
				CKmito ^{oe} sham vs. CKmito ^{oe} TAC (11 vs. 8)	ns	0.244
				WT sham vs. CKmito ^{oe} sham (10 vs. 11)	ns	0.272
				WT TAC vs. CKmito ^{oe} TAC (10 vs. 8)	ns	0.864
Fig. 6B	No	Kruskal-Wallis test	pair-wise, two-sided multiple comparison analysis (Dunn method with Benjamini-Hochberg adjustment for multiple comparisons)	WT sham vs. WT TAC (5 vs. 6)	*	0.020
				CKmyofib ^{oe} sham vs. CKmyofib ^{oe} TAC (5 vs. 6)	*	0.040
				WT sham vs. CKmyofib ^{oe} sham (5 vs. 5)	ns	0.368
				WT TAC vs. CKmyofib ^{oe} TAC (6 vs. 6)	ns	0.477

Online Fig. 1A	Yes	two-tailed Student's <i>t</i> -test	N/A	WT LV vs. CKmito ^{oe} LV (5 vs. 5)	ns	0.392
	Yes	two-tailed Student's <i>t</i> -test	N/A	WT Atria vs. CKmito ^{oe} Atria (5 vs. 5)	ns	0.977
Online Fig. 1A (non-parametric alternative)		Wilcoxon signed rank test	N/A	WT LV vs. CKmito ^{oe} LV (5 vs. 5)	ns	0.392
		Wilcoxon signed rank test	N/A	WT Atria vs. CKmito ^{oe} Atria (5 vs. 5)	ns	0.977
Online Fig. 1B	Yes	two-tailed Student's <i>t</i> -test	N/A	WT LV vs. CKmito ^{oe} LV (5 vs. 5)	ns	0.422
	No	Wilcoxon signed rank test	N/A	WT Atria vs. CKmito ^{oe} Atria (5 vs. 5)	ns	0.399

Online Fig. 1B (non-parametric alternative)		Wilcoxon signed rank test	N/A	WT LV vs. CKmito ^{oe} LV (5 vs. 5)	ns	0.422
Online Fig. 1D	Yes	two-way ANOVA	Tukey's multiple comparisons test	WT sham vs. WT TAC (5 vs. 8)	**	0.0023
				CKmito ^{oe} sham vs. CKmito ^{oe} TAC (5 vs. 8)	ns	0.053
				WT sham vs. CKmito ^{oe} sham (5 vs. 5)	ns	0.747
				WT TAC vs. CKmito ^{oe} TAC (8 vs. 8)	ns	0.242
Online Fig. 1D (non-parametric alternative)		Kruskal-Wallis test	pair-wise, two-sided multiple comparison analysis (Dunn method with Benjamini-Hochberg adjustment for multiple comparisons)	WT sham vs. WT TAC (5 vs. 8)	*	0.021
				CKmito ^{oe} sham vs. CKmito ^{oe} TAC (5 vs. 8)	ns	0.113
				WT sham vs. CKmito ^{oe} sham (5 vs. 5)	ns	0.741
				WT TAC vs. CKmito ^{oe} TAC (8 vs. 8)	ns	0.453
Online Fig. 1E	Yes	two-way ANOVA	Tukey's multiple comparisons test	WT sham vs. WT TAC (5 vs. 8)	*	0.021
				CKmito ^{oe} sham vs. CKmito ^{oe} TAC (5 vs. 8)	ns	0.754
				WT sham vs. CKmito ^{oe} sham (5 vs. 5)	ns	0.436
				WT TAC vs. CKmito ^{oe} TAC (8 vs. 8)	ns	0.157
Online Fig. 1E (non-parametric alternative)		Kruskal-Wallis test	pair-wise, two-sided multiple comparison analysis (Dunn method with Benjamini-Hochberg adjustment for multiple comparisons)	WT sham vs. WT TAC (5 vs. 8)	ns	0.147
				CKmito ^{oe} sham vs. CKmito ^{oe} TAC (5 vs. 8)	ns	0.890
				WT sham vs. CKmito ^{oe} sham (5 vs. 5)	ns	0.564
				WT TAC vs. CKmito ^{oe} TAC (8 vs. 8)	ns	0.354
Online Fig. 1F	Yes	two-way ANOVA	Tukey's multiple comparisons test	WT sham vs. WT TAC (5 vs. 8)	***	0.00027
				CKmito ^{oe} sham vs. CKmito ^{oe} TAC (5 vs. 8)	**	0.0065
				WT sham vs. CKmito ^{oe} sham (5 vs. 5)	ns	0.997
				WT TAC vs. CKmito ^{oe} TAC (8 vs. 8)	ns	0.080
Online Fig. 1F (non-parametric alternative)		Kruskal-Wallis test	pair-wise, two-sided multiple comparison analysis (Dunn method with Benjamini-Hochberg adjustment for multiple comparisons)	WT sham vs. WT TAC (5 vs. 8)	*	0.0077
				CKmito ^{oe} sham vs. CKmito ^{oe} TAC (5 vs. 8)	*	0.022
				WT sham vs. CKmito ^{oe} sham (5 vs. 5)	ns	0.901
				WT TAC vs. CKmito ^{oe} TAC (8 vs. 8)	ns	0.566
Online Fig. 1G	Yes	two-way ANOVA	Tukey's multiple comparisons test	WT sham vs. WT TAC (5 vs. 8)	***	0.00014
				CKmito ^{oe} sham vs. CKmito ^{oe} TAC (5 vs. 8)	***	0.00072

				WT sham vs. CKmito ^{oe} sham (5 vs. 5)	ns	0.490
				WT TAC vs. CKmito ^{oe} TAC (8 vs. 8)	*	0.022
Online Fig. 1G (non-parametric alternative)		Kruskal-Wallis test	pair-wise, two-sided multiple comparison analysis (Dunn method with Benjamini-Hochberg adjustment for multiple comparisons)	WT sham vs. WT TAC (5 vs. 8)	***	0.0010
				CKmito ^{oe} sham vs. CKmito ^{oe} TAC (5 vs. 8)	*	0.041
				WT sham vs. CKmito ^{oe} sham (5 vs. 5)	ns	0.535
				WT TAC vs. CKmito ^{oe} TAC (8 vs. 8)	ns	0.392
Online Fig. 1H	Yes	two-way ANOVA	Tukey's multiple comparisons test	WT sham vs. WT TAC (5 vs. 8)	***	0.00018
				CKmito ^{oe} sham vs. CKmito ^{oe} TAC (5 vs. 8)	ns	0.063
				WT sham vs. CKmito ^{oe} sham (5 vs. 5)	ns	0.323
				WT TAC vs. CKmito ^{oe} TAC (8 vs. 8)	*	0.031
Online Fig. 1H (non-parametric alternative)		Kruskal-Wallis test	pair-wise, two-sided multiple comparison analysis (Dunn method with Benjamini-Hochberg adjustment for multiple comparisons)	WT sham vs. WT TAC (5 vs. 8)	***	0.0010
				CKmito ^{oe} sham vs. CKmito ^{oe} TAC (5 vs. 8)	ns	0.139
				WT sham vs. CKmito ^{oe} sham (5 vs. 5)	ns	0.339
				WT TAC vs. CKmito ^{oe} TAC (8 vs. 8)	ns	0.311
Online Fig. 2A	Yes	two-tailed Student's <i>t</i> -test	N/A	WT TAC vs. GAMT ^{-/-} TAC (7 vs. 4)	ns	0.244
Online Fig. 2A (non-parametric alternative)		Mann-Whitney test	N/A	WT TAC vs. GAMT ^{-/-} TAC (7 vs. 4)	ns	0.527
Online Fig. 2B	Yes	two-tailed Student's <i>t</i> -test	N/A	WT TAC vs. GAMT ^{-/-} TAC (7 vs. 4)	ns	0.220
Online Fig. 2B (non-parametric alternative)		Mann-Whitney test	N/A	WT TAC vs. GAMT ^{-/-} TAC (7 vs. 4)	ns	0.315
Online Fig. 2C	Yes	two-tailed Student's <i>t</i> -test	N/A	WT TAC vs. GAMT ^{-/-} TAC (7 vs. 4)	ns	0.060
Online Fig. 2C (non-parametric alternative)		Mann-Whitney test	N/A	WT TAC vs. GAMT ^{-/-} TAC (7 vs. 4)	ns	0.315
Online Fig. 2D	Yes	two-tailed Student's <i>t</i> -test	N/A	WT TAC vs. GAMT ^{-/-} TAC (7 vs. 4)	***	0.0028
Online Fig. 2D (non-parametric alternative)		Mann-Whitney test	N/A	WT TAC vs. GAMT ^{-/-} TAC (7 vs. 4)	**	0.006
Online Fig. 2E	Yes	two-tailed Student's <i>t</i> -test	N/A	WT TAC vs. GAMT ^{-/-} TAC (7 vs. 4)	ns	0.072
Online Fig. 2D (non-parametric alternative)		Mann-Whitney test		WT TAC vs. GAMT ^{-/-} TAC (7 vs. 4)	ns	0.073

Online Fig. 2F	No	Kruskal-Wallis test	pair-wise, two-sided multiple comparison analysis (Dunn method with Benjamini-Hochberg adjustment for multiple comparisons)	GAMT ^{-/-} x WT sham vs. GAMT ^{-/-} x WT TAC (2 vs. 8)	ns	1.00
				GAMT ^{-/-} x CKmito ^{oe} sham vs. GAMT ^{-/-} x CKmito ^{oe} TAC (2 vs. 5)	ns	0.975
				GAMT ^{-/-} x WT sham vs. GAMT ^{-/-} x CKmito ^{oe} sham (2 vs. 2)	ns	0.842
				GAMT ^{-/-} x WT TAC vs. GAMT ^{-/-} x CKmito ^{oe} TAC (8 vs. 5)	ns	1.00
Online Fig. 2G	Yes	two-tailed Student's <i>t</i> -test	N/A	WT sham vs. GAMT ^{-/-} x WT sham (10 vs. 5)	**	0.0079
				WT TAC vs. GAMT ^{-/-} x WT TAC (13 vs. 8)	**	0.0045
				CKmito ^{oe} sham vs. GAMT ^{-/-} x CKmito ^{oe} sham (10 vs. 5)	ns	0.112
				CKmito ^{oe} TAC vs. GAMT ^{-/-} x CKmito ^{oe} TAC (13 vs. 5)	**	0.0061
Online Fig. 2G (non-parametric alternative)		Wilcoxon signed rank test	N/A	WT sham vs. GAMT ^{-/-} x WT sham (10 vs. 5)	**	0.0079
				WT TAC vs. GAMT ^{-/-} x WT TAC (13 vs. 8)	ns	0.077
				CKmito ^{oe} sham vs. GAMT ^{-/-} x CKmito ^{oe} sham (10 vs. 5)	ns	0.112
				CKmito ^{oe} TAC vs. GAMT ^{-/-} x CKmito ^{oe} TAC (13 vs. 5)	**	0.0061
Online Fig. 3A	No	Wilcoxon signed rank test	pairwise, two-sided multiple comparison analysis (Dwass, Steel, Crichlow-Fligner Method)	WT sham vs. WT TAC (8 vs. 8)	*	0.032
				CKmito ^{oe} sham vs. CKmito ^{oe} TAC (9 vs. 10)	ns	0.806
				WT sham vs. CKmito ^{oe} sham (8 vs. 9)	ns	0.771
				WT TAC vs. CKmito ^{oe} TAC (8 vs. 10)	**	0.010
Online Fig. 3B	No	Kruskal-Wallis test	pair-wise, two-sided multiple comparison analysis (Dunn method with Benjamini-Hochberg adjustment for multiple comparisons)	WT sham vs. WT TAC (6 vs. 7)	ns	0.230
				CKmyofib ^{oe} sham vs. CKmyofib ^{oe} TAC (5 vs. 7)	ns	0.832
				WT sham vs. CKmyofib ^{oe} sham (6 vs. 5)	ns	0.264
				WT TAC vs. CKmyofib ^{oe} TAC (7 vs. 7)	*	0.020
Online Fig. 3C	Yes	two-way ANOVA	Tukey's multiple comparisons test	WT sham vs. WT TAC (7 vs. 6)	*	0.020
				CKmito ^{oe} sham vs. CKmito ^{oe} TAC (7 vs. 7)	ns	0.673
				WT sham vs. CKmito ^{oe} sham (7 vs. 7)	ns	0.706
				WT TAC vs. CKmito ^{oe} TAC (6 vs. 7)	ns	0.111
Online Fig. 3D	Yes	two-way ANOVA	Tukey's multiple comparisons test	WT sham vs. WT TAC (5 vs. 8)	*	0.022
				CKmyofib ^{oe} sham vs. CKmyofib ^{oe} TAC (6 vs. 7)	ns	0.657

				WT sham vs. CKmyofib ^{oe} sham (5 vs. 6)	ns	0.636
				WT TAC vs. CKmyofib ^{oe} TAC (8 vs. 7)	*	0.015
Online Fig. 3D (non-parametric alternative)		Kruskal-Wallis test	pair-wise, two-sided multiple comparison analysis (Dunn method with Benjamini-Hochberg adjustment for multiple comparisons)	WT sham vs. WT TAC (5 vs. 8)	ns	0.650
				CKmyofib ^{oe} sham vs. CKmyofib ^{oe} TAC (6 vs. 7)	ns	0.125
				WT sham vs. CKmyofib ^{oe} sham (5 vs. 6)	ns	0.566
				WT TAC vs. CKmyofib ^{oe} TAC (8 vs. 7)	ns	0.15
Online Fig. 3E	Yes	two-way ANOVA	Tukey's multiple comparisons test	WT sham vs. WT TAC (7 vs. 6)	ns	0.102
				CKmito ^{oe} sham vs. CKmito ^{oe} TAC (7 vs. 7)	ns	0.469
				WT sham vs. CKmito ^{oe} sham (7 vs. 7)	ns	0.079
				WT TAC vs. CKmito ^{oe} TAC (6 vs. 7)	**	0.0092
Online Fig. 3F	No	Kruskal-Wallis test	pair-wise, two-sided multiple comparison analysis (Dunn method with Benjamini-Hochberg adjustment for multiple comparisons)	WT sham vs. WT TAC (6 vs. 7)	ns	0.198
				CKmyofib ^{oe} sham vs. CKmyofib ^{oe} TAC (5 vs. 7)	ns	0.231
				WT sham vs. CKmyofib ^{oe} sham (6 vs. 5)	ns	0.627
				WT TAC vs. CKmyofib ^{oe} TAC (7 vs. 7)	**	0.0022
Online Fig. 4A	Yes	two-way ANOVA	Tukey's multiple comparisons test	WT sham vs. WT TAC (7 vs. 7)	***	0.00072
				CKmito ^{oe} sham vs. CKmito ^{oe} TAC (6 vs. 7)	**	0.0012
				WT sham vs. CKmito ^{oe} sham (7 vs. 6)	ns	0.861
				WT TAC vs. CKmito ^{oe} TAC (7 vs. 7)	ns	0.791
Online Fig. 4C	No	Kruskal-Wallis test	pair-wise, two-sided multiple comparison analysis (Dunn method with Benjamini-Hochberg adjustment for multiple comparisons)	WT sham vs. WT TAC (6 vs. 4)	ns	1.00
				CKmito ^{oe} sham vs. CKmito ^{oe} TAC (6 vs. 5)	ns	0.674
				WT sham vs. CKmito ^{oe} sham (6 vs. 6)	ns	1.00
				WT TAC vs. CKmito ^{oe} TAC (4 vs. 5)	ns	0.938
Online Fig. 4D	Yes	two-way ANOVA	Tukey's multiple comparisons test	WT sham vs. WT TAC (6 vs. 4)	ns	0.415
				CKmito ^{oe} sham vs. CKmito ^{oe} TAC (6 vs. 5)	ns	0.081
				WT sham vs. CKmito ^{oe} sham (6 vs. 6)	ns	0.334
				WT TAC vs. CKmito ^{oe} TAC (4 vs. 5)	ns	0.987
Online Fig. 4D (non-parametric alternative)		Kruskal-Wallis test	pair-wise, two-sided multiple comparison analysis (Dunn)	WT sham vs. WT TAC (6 vs. 4)	ns	0.447
				CKmito ^{oe} sham vs. CKmito ^{oe} TAC (6 vs. 5)	ns	0.551

			method with Benjamini-Hochberg adjustment for multiple comparisons)	WT sham vs. CKmito ^{oe} sham (6 vs. 6)	ns	0.654
				WT TAC vs. CKmito ^{oe} TAC (4 vs. 5)	ns	1.00
Online Fig. 4F	No	Wilcoxon signed rank test	N/A	WT sham vs. WT TAC (6 vs. 7)	ns	
				CKmito ^{oe} sham vs. CKmito ^{oe} TAC (6 vs. 7)	ns	
				WT sham vs. CKmito ^{oe} sham (6 vs. 6)	ns	
				WT TAC vs. CKmito ^{oe} TAC (7 vs. 7)	ns	
Online Fig. 4G	Yes	two-way ANOVA	Tukey's multiple comparisons test	WT sham vs. WT TAC (6 vs. 7)	ns	0.557
				CKmito ^{oe} sham vs. CKmito ^{oe} TAC (6 vs. 7)	ns	0.445
				WT sham vs. CKmito ^{oe} sham (6 vs. 6)	ns	0.682
				WT TAC vs. CKmito ^{oe} TAC (7 vs. 7)	ns	0.528
Online Fig. 4I	Yes	two-way ANOVA	Tukey's multiple comparisons test	WT sham vs. WT TAC (7 vs. 7)	ns	0.069
				CKmito ^{oe} sham vs. CKmito ^{oe} TAC (6 vs. 6)	ns	0.351
				WT sham vs. CKmito ^{oe} sham (7 vs. 6)	*	0.027
				WT TAC vs. CKmito ^{oe} TAC (7 vs. 6)	ns	0.141
Online Fig. 4J	No	Wilcoxon signed rank test	pairwise, two-sided multiple comparison analysis (Dwass, Steel, Crichlow-Fligner Method)	WT sham vs. WT TAC (7 vs. 7)	ns	0.380
				CKmito ^{oe} sham vs. CKmito ^{oe} TAC (6 vs. 6)	*	0.021
				WT sham vs. CKmito ^{oe} sham (7 vs. 6)	ns	0.247
				WT TAC vs. CKmito ^{oe} TAC (7 vs. 6)	*	0.014
Online Fig. 5A	Yes	two-way ANOVA	Tukey's multiple comparisons test	WT sham vs. WT TAC (10 vs. 13)	***	0.00092
				CKmyofib ^{oe} sham vs. CKmyofib ^{oe} TAC (11 vs. 14)	ns	0.339
				WT sham vs. CKmyofib ^{oe} sham (10 vs. 11)	ns	0.490
				WT TAC vs. CKmyofib ^{oe} TAC (13 vs. 14)	*	0.038
Online Fig. 5B	Yes	two-way ANOVA	Tukey's multiple comparisons test	WT sham vs. WT TAC (5 vs. 7)	ns	0.432
				CKmyofib ^{oe} sham vs. CKmyofib ^{oe} TAC (6 vs. 7)	***	0.00027
				WT sham vs. CKmyofib ^{oe} sham (5 vs. 6)	***	0.00047
				WT TAC vs. CKmyofib ^{oe} TAC (7 vs. 7)	ns	0.381
Online Fig. 5B (non-parametric alternative)		Kruskal-Wallis test	pair-wise, two-sided multiple comparison analysis (Dunn method with Benjamini-Hochberg	WT sham vs. WT TAC (5 vs. 7)	ns	0.715
				CKmyofib ^{oe} sham vs. CKmyofib ^{oe} TAC (6 vs. 7)	*	0.044
				WT sham vs. CKmyofib ^{oe} sham (5 vs. 6)	*	0.026

			adjustment for multiple comparisons)	WT TAC vs. CKmyofib ^{oe} TAC (7 vs. 7)	ns	0.490
Online Fig. 5C	Yes	two-way ANOVA	Tukey's multiple comparisons test	WT sham vs. WT TAC (3 vs. 5)	***	0.00077
				CKmyofib ^{oe} sham vs. CKmyofib ^{oe} TAC (3 vs. 4)	ns	0.279
				WT sham vs. CKmyofib ^{oe} sham (3 vs. 3)	ns	1.000
				WT TAC vs. CKmyofib ^{oe} TAC (3 vs. 4)	**	0.0028
Online Fig. 5C (non-parametric alternative)		Kruskal-Wallis test	pair-wise, two-sided multiple comparison analysis (Dunn method with Benjamini-Hochberg adjustment for multiple comparisons)	WT sham vs. WT TAC (3 vs. 5)	ns	0.057
				CKmyofib ^{oe} sham vs. CKmyofib ^{oe} TAC (3 vs. 4)	ns	0.377
				WT sham vs. CKmyofib ^{oe} sham (3 vs. 3)	ns	0.584
				WT TAC vs. CKmyofib ^{oe} TAC (3 vs. 4)	ns	0.111
Online Fig. 5D	Yes	two-way ANOVA	Tukey's multiple comparisons test	WT sham vs. WT TAC (3 vs. 5)	ns	0.282
				CKmyofib ^{oe} sham vs. CKmyofib ^{oe} TAC (3 vs. 4)	ns	0.291
				WT sham vs. CKmyofib ^{oe} sham (3 vs. 3)	*	0.039
				WT TAC vs. CKmyofib ^{oe} TAC (3 vs. 4)	ns	0.050
Online Fig. 5D (non-parametric alternative)		Kruskal-Wallis test	pair-wise, two-sided multiple comparison analysis (Dunn method with Benjamini-Hochberg adjustment for multiple comparisons)	WT sham vs. WT TAC (3 vs. 5)	ns	0.307
				CKmyofib ^{oe} sham vs. CKmyofib ^{oe} TAC (3 vs. 4)	ns	0.522
				WT sham vs. CKmyofib ^{oe} sham (3 vs. 3)	ns	0.235
				WT TAC vs. CKmyofib ^{oe} TAC (3 vs. 4)	ns	0.171
Online Fig. 5E	No	generalized estimating equation model to take into account the correlation of within-subject data		WT sham vs. WT TAC (20 cells (from 6 mice) vs. 6 cells (from 2 mice))	***	0.00050
				CKmyofib ^{oe} sham vs. CKmyofib ^{oe} TAC (17 cells (from 4 mice) vs. 7 cells (from 2 mice))	***	< 0.00010
				WT sham vs. CKmyofib ^{oe} sham (20 cells (from 6 mice) vs. 17 cells (from 4 mice))	**	0.0040
				WT TAC vs. CKmyofib ^{oe} TAC (6 cells (from 2 mice) vs. 7 cells (from 2 mice))	****	< 0.00010